A NEW APPROACH TO BITUMINOUS COMPOSITES

A THESIS SUBMITTED TO
THE GRADUATE SCHOOL OF NATURAL AND APPLIED SCIENCES
OF
MIDDLE EAST TECHNICAL UNIVERSITY

BY

DİLEK OKUŞ

IN PARTIAL FULFILLMENT OF THE REQUIREMENTS
FOR
THE DEGREE OF MASTER OF SCIENCE
IN
CHEMISTRY

JULY 2010

Approval of the thesis:

A NEW APPROACH TO BITUMINOUS COMPOSITES

submitted by **DİLEK OKUŞ** in partial fulfillment of the requirements for the degree of **Master of Sciences in Chemistry, Middle East Technical University** by,

Prof. Dr. Canan Özgen
Dean, Graduate School of **Natural and Applied Sciences**

Prof. Dr. İlker Özkan
Head of Department, **Chemistry**

Prof. Dr. Teoman Tinçer
Supervisor, **Chemistry Dept., METU**

Examining Committee Members:

Prof. Dr. Leyla Aras
Chemistry Dept., METU

Prof. Dr. Teoman Tinçer
Chemistry Dept., METU

Prof. Dr. Ali Usanmaz
Chemistry Dept., METU

Prof. Dr. Savaş Küçükyavuz
Chemistry Dept., METU

Prof. Dr. Ülkü Yılmazer
Chemical Engineering Dept., METU

Date: 02.07.2010

I hereby declare that all information in this document has been obtained and presented in accordance with academic rules and ethical conduct. I also declare that, as required by these rules and conduct, I have fully cited and referenced all material and results that are not original to this work.

Name, Last Name : Dilek OKUŞ

Signature :

ABSTRACT

A NEW APPROACH TO BITUMINOUS COMPOSITES

Okuş, Dilek
M.Sc., Department of Chemistry
Supervisor: Prof. Dr. Teoman Tinçer

July 2010, 67 pages

The healing effects of fillers on bitumen have been known for many years. In this study, the effects of fillers, e.g. manganese dioxide, barium sulfate, perlite and vermiculite, and filler concentrations on morphological, mechanical, flow and sound insulation characteristics of bitumen were examined. It was also aimed to improve the mechanical and sound insulation properties of bituminous composites.

Bituminous composites were prepared by using Brabender Plasti-Corder. Mixing was made at 130°C with 60 rpm for 20 minutes. 20/30 and 50/70 penetration grades bitumen, SBS polymer and CaO used in the composites were kept constant. While the amount of $CaCO_3$ was decreased, other fillers (i.e., MnO_2, $BaSO_4$, perlite and vermiculite) were added in the same proportion to investigate their effects.

According to the test results, all fillers were covered by bitumen as observed in SEM figures. MnO_2 composites did not give good results in the tests and they were very brittle. While perlite seemed to have good mechanical properties, it was too viscous to be processed easily. Increase in the amount of vermiculite in the composite caused adverse effects on the rheological properties of composites. However, vermiculite composites provided a remarkable sound insulation in terms of the sound damping ratios. $BaSO_4$ composites gave the best results in the mechanical, flow and sound insulation tests.

Keywords: Bitumen, bituminous composites, asphalt, fillers

ÖZ

BİTÜM KARIŞIMLARINA YENİ BİR YAKLAŞIM

Okuş, Dilek
Yüksek Lisans, Kimya
Tez Yöneticisi: Prof. Dr. Teoman Tinçer

Temmuz 2010, 67 sayfa

Dolgu malzemelerinin bitüm üzerindeki iyileştirici etkileri yıllardan beri bilinmektedir. Bu çalışmada mangan dioksit, baryum sülfat, perlit ve vermikülit dolgu malzemelerinin cinsinin ve oranının bitümün morfolojik, mekanik, akışkanlık ve ses yalıtımı üzerindeki etkisi incelenmiştir. Aynı zamanda, iyi mekanik ve ses yalıtım özelliklerine sahip bitüm karışımı geliştirmek amaçlanmıştır.

Bitüm karışımları Brabender Plasti-Corder kullanılarak hazırlanmıştır. Karıştırma işlemi 20 dakika boyunca 60 devir/dakika ile 130ºC'de yapılmıştır. Karışımlarda kullanılan 20/30 ve 50/70 penetrasyonlu bitüm, SBS polimer ve CaO oranları sabit tutulmuştur. Dolgu malzemelerinin bitüm üzerindeki etkilerini anlamak için, $CaCO_3$ ana dolgu malzemesi azaltılarak yerine MnO_2, $BaSO_4$, perlit ve vermikülit eklenerek yeni karışımlar oluşturulmuştur.

Test sonuçlarına göre, dolgu malzemelerinin bitüm tarafından kaplandığı SEM fotoğraflarında görülmüştür. MnO_2 karışımları testlerde iyi sonuçlar vermemiştir ve çok kırılgan bir yapıya sahiptirler. Perlit mekanik açıdan iyi görünse de çok akmaz bir yapıya sahip olduğundan işlenebilmesi zordur. Karışımdaki vermikülit miktarının artışı reolojik özellikleri kötü etkilemektedir. Fakat ses sönüm oranları açısından vermikülit karışımları dikkate değer bir ses yalıtımı sağlamaktadır. $BaSO_4$ karışımları mekanik, akışkanlık ve ses yalıtım testlerinde en iyi sonuçları vermiştir.

Anahtar Kelimeler: Bitüm, bitüm karışımları, asfalt, dolgu malzemeleri

To my family

ACKNOWLEDGEMENTS

I would like to express my deepest gratitude to my thesis supervisor Prof. Dr. Teoman Tinçer for his guidance, understanding, kind support, encouraging advices, criticism, and valuable discussions throughout my thesis.

I would like to thank Yunus Karataş, Tuğba Efe and Binnur Özkan for their help, cooperation and friendship.

My deepest appreciation is for my best friends Özlem Karakaş and Esma Yıldırım. During this work, they have always motivated me with their friendship, help, and understanding.

Special thanks go to ARÇELİK for their support through this work. I would also like to thank to Çağlar Yazgan Balçık and Ahmet Ali Uslu for Oberst Test analysis.

Finally, I wish to express my sincere thanks to my family since without their love, advice, care, and support this work would not be possible. My family's absolute unquestionable belief in me has been a constant source of encouragement and has helped me achieving my goals.

TABLE OF CONTENTS

CHAPTERS

APPENDICES

LIST OF TABLES

TABLES

LIST OF FIGURES

FIGURES

CHAPTER 1

INTRODUCTION

1.1 Bitumen

1.1.1 Definition of Bitumen

Bitumen which is a naturally occurring substance is a black or dark brown highly viscous liquid or semisolid material. Crude oil and natural deposit are the sources of bitumen [1]. In the American terminology, bitumen and asphalt are synonyms and the term “asphalt” is at most of the instances used instead of bitumen. However, in Europe, asphalt consists of natural bitumen and mineral matter, and “bitumen” or “asphaltic bitumen” is used mostly [2, 3]. Bitumen is a mixture of hydrocarbons and free from oxygenated bodies [4]. Bitumen is a water insoluble substance, however, it is partially soluble in aliphatic organic solvents and soluble in carbon disulfide, chloroform, acetone and ether [5].

Bitumen is obtained from crude oil that contains the residual of marine organisms and vegetable matter [6]. Crude oil composed of hydrocarbons can be decomposed by fractional distillation because of the difference in boiling points of hydrocarbons. As it is shown in Figure 1.1, bitumen can be obtained as a heavy residue by subjecting crude oil to a controlled fractional distillation or refinement that removes the volatile components [7]. The term “bituminous substance” is used to describe the substance including bitumen.

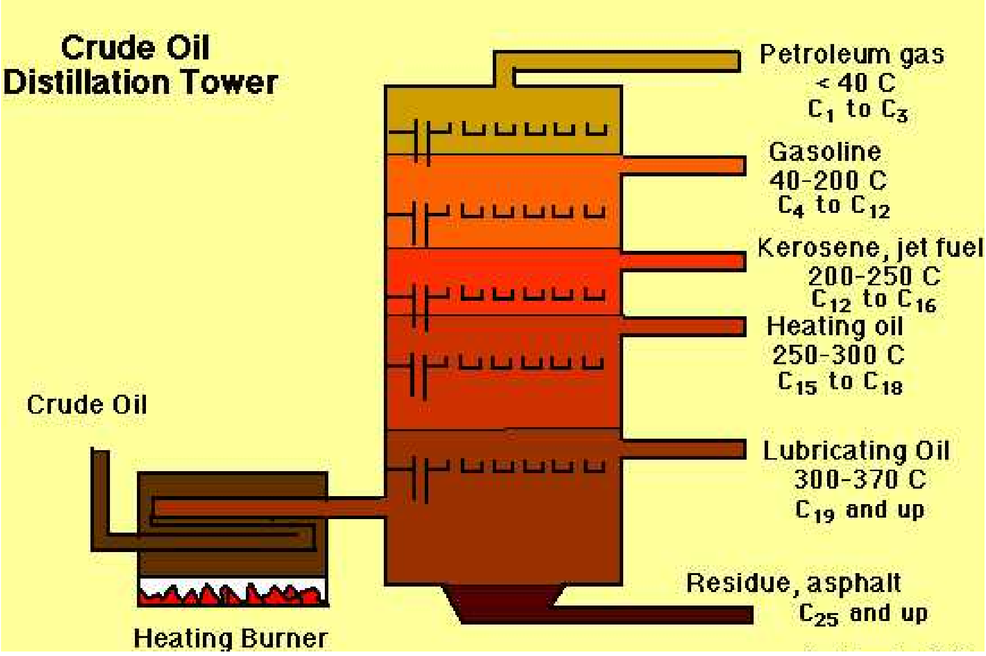

Figure 1.1 Fractional distillation of crude oil [8].

1.1.2 Chemical Composition of Bitumen

Element analysis of bitumen indicates that besides hydrocarbon groups, bitumen consists of sulphur, oxygen and nitrogen atoms and trace quantities of metals such as vanadium, magnesium, calcium, nickel and iron. These metals exist in the form of inorganic salts and oxides in the structure of bitumen [9]:

Carbon : 82 – 88 %
Hydrogen: 8 – 11 %
Sulphur : 0 – 6 %
Oxygen: 0 – 1.5 %
Nitrogen: 0 – 1%

Hydrocarbons, being the main components of bitumen, can easily react with oxygen, thus, they change the chemical structure of bitumen resulting in cracks [10].

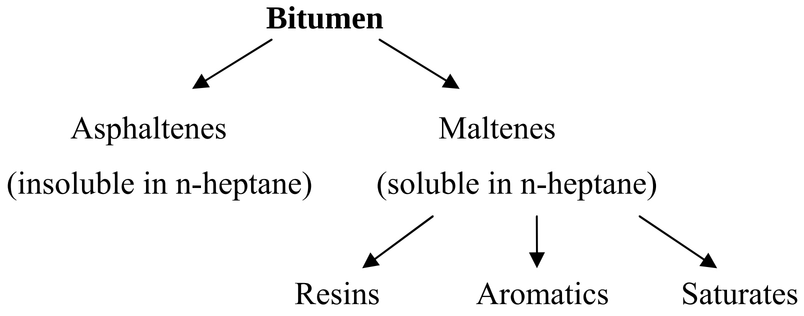

Figure 1.2 Components of bitumen [10].

Bitumen which is a complex mixture of organic and inorganic compounds can be divided into asphaltenes and maltenes [11]. Asphaltenes, high molecular weight amorphous solids, are black, highly polar and insoluble in *n*-heptane. Asphaltene content affects the bitumen rheology. Increase in asphaltene content makes bitumen harder and more viscous [9].

Maltenes, made up of saturates, aromatics and resins, are soluble in *n*-heptane [11]. While saturated and aromatic compounds are viscous liquids, resins are semi-solid substances which give an adhesive character to the bitumen [12]. High molecular weight asphaltenes dissolve in a lower molecular weight maltenes [6].

1.1.3 Physical and Chemical Properties of Bitumen

Bitumen can be considered as a low molecular weight natural polymer [13]. The number-average molecular weight is between 600 and 1500 g/mol. However, the distribution extends to molecular weights up to 15000 g/mol [2]. Like all polymers, bitumen is a viscoelastic material so it is particularly temperature susceptible. Bitumen is rigid and brittle at low temperatures, flexible at room temperature, and fluid at higher temperatures [13]. Under an applied load, permanent deformation occurs. The rate of deformation depends on the bitumen grade, asphalt constitution, ambient temperature, and level of stress and load time [7].

Bitumen density at room temperature is between 1.01 and 1.04 g/cm^3 and it depends on the crude source and paving grade [2]. The bitumen density increases when penetration decreases and softening point increases [3]. Bitumen exhibits two glass transition temperatures at −20 °C assigned to maltenes and 70°C to the asphaltenes [13].

Bitumen shows a good resistance against acids depending on the acid concentration. While bitumen is not affected by dilute acids, highly concentrated one can react with it [3]. Bitumen is involatile and adhesive [2]. Due to its adhesive, viscous and ductile character, bitumen resists water and vapor penetration [14].

1.1.4 Uses of Bitumen

Bitumen-based composites have been used since ancient times. The ancient Egyptians preserved the mummies with bitumen during the Ptolemaic period [6]. Today, bitumen is mostly used in the construction of roadways and runways because of its durability [15]. Bitumen is also used as a binder due to its adhesive character. For example, it is used to paste the bricks in road construction [10].

Moreover, bitumen is used as an insulator in electrical appliances such as transformers and cables [15]. It shows good resistance to the high energy radiation so it is used to store and transport low and moderately radioactive wastes [6]. Bitumen is used as sound insulating material in buildings, automobiles, household appliances [16] such as washing machines, dishwashers, tumble dryers etc. [6]. By the modification with polymers, bitumen can be also used as waterproof material in roofs, terraces etc. [16].

1.2 Additives

For the modifiers or additives to be effective, and for their uses to be practicable and economic, they must [6]:

- be easily available
- show resistance to degradation at process and application temperatures
- mix with bitumen well

- resist to flow at high temperatures not to make bitumen too viscous at application temperatures and not to make it too stiff at low temperatures
- be economic

The modifier mixed with bitumen should show the following characteristics [6]:

- maintain its properties and be stable during storage, application and in service
- be able to be processed with conventional equipments
- have a coating viscosity at normal application temperatures

The effects of polymer additives and fillers on bitumen are shown in Table 1.1. [6]

Modifier	Property affected
APA (Atactic polypropylene) EVA (Ethylene vinyl acetate)	Stiffness Penetration value Softening point Fraass breaking point
SBS (Styrene butadiene styrene)	Penetration value Softening point Elastic recovery Brittleness at low temperature
Filler powders	Softening point Stiffness Viscosity Density Mechanical strength Cost

Table 1.1 The relationship between final property of modified bitumen and some modifiers

1.2.1 Polymer Additives

Polymers are used as additives to improve the properties of bitumen. Polymer addition, even in small amounts, affects the rheological characteristics of bitumen [17]. The purpose of using polymers is essentially to make bitumen more elastic, to reduce the risk of permanent deformation caused by viscous flow under applied loading and to improve the strength [7].

Plastics can be divided into two groups. Thermoplastics soften when heated and become tough when cooled and can be repeated. Thermosets cannot be reshaped readily. For the bitumen modifications, thermoplastics are more useful. Thermoplastics can be grouped as plastics and elastomers [12]. Plastics used in bitumen modification are polyethylene, polypropylene, ethylene vinyl acetate (EVA), ethylene methyl acrylate (EMA) and polyvinyl chloride (PVC) [12]. EVA is the most commonly used plastics. While others make bitumen too stiff and brittle, it hardens bitumen and makes it more resistant to loading and rutting [7]. On the other hand, elastomers which are the most usually used polymers in the bitumen modifications are natural rubber or latex, synthetic rubber, styrene butadiene styrene (SBS), styrene butadiene rubber (SBR), styrene ethylene butadiene styrene (SEBS) and polybutadiene, polychloroprene, polyisoprene [12].

Elastomers increase the elasticity and improve the ductility of bitumen, while plastics make bitumen harder. Elastomers reduce the temperature sensitivity of bitumen, and so they decrease the risk of rutting at high temperatures, whereas plastomers are less successful to reduce the risk [7]. At present, styrene butadiene styrene (SBS) is the most commonly used polymer in the modification of bitumen. Other polymers such as styrene butadiene rubber, ethylene vinyl acetate and polyethylene are also used mostly [18].

1.2.1.1 Styrene Butadiene Styrene (SBS) Block Copolymer

SBS block copolymer is the most commonly used polymer in the bitumen modifications. It belongs to the A-B-A type thermoplastic elastomers. In this type of structure, thermoplastic rubber groups are terminated by the hard, glassy end blocks. As it is seen in Figure 1.3, SBS encloses polystyrene components attached to polybutadiene [19].

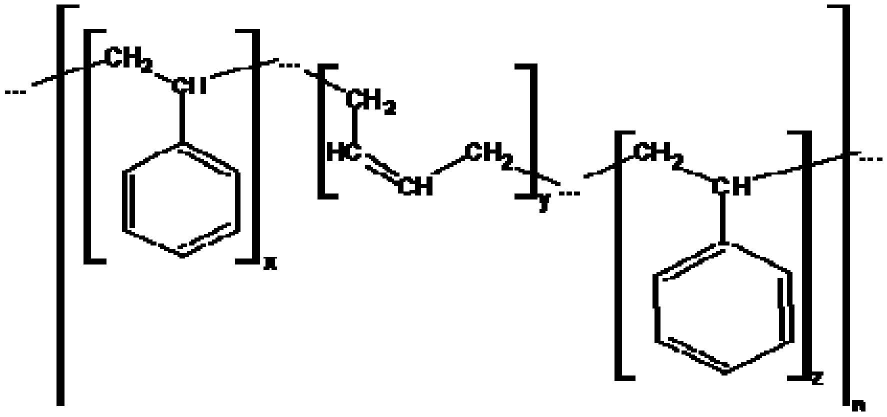

Figure 1.3 Structure of styrene butadiene styrene (SBS)

SBS polymer obtains its strength and elasticity from physical cross-linking of the molecules into a three-dimensional network. Polystyrene parts give the polymer its strength, and polybutadiene parts enhance the elasticity of the compound [18].

SBS, like elastomeric polymers, enhances the elasticity and reduces the viscosity of bituminous composites. Therefore, it also reduces the risk of deformation or cracking. Moreover, SBS is the most favorable for bitumen modification in terms of performance, endurance, ease of use and economy [7].

SBS is not a reactive material so that it cannot chemically interact with the bitumen and they form a binary system. A more stable binary system takes place when the two phases are more homogeneous [20]. When SBS polymer is mixed with bitumen, asphaltenes are less prone to blend with it, however, oil fractions or maltenes are absorbed by the elastomeric phase (or polybutadiene parts) of SBS (Figure 1.4). This results in a swelling of polymer up to nine times of its initial volume and a continuous polymer phase that affects the bitumen rheology [21, 22].

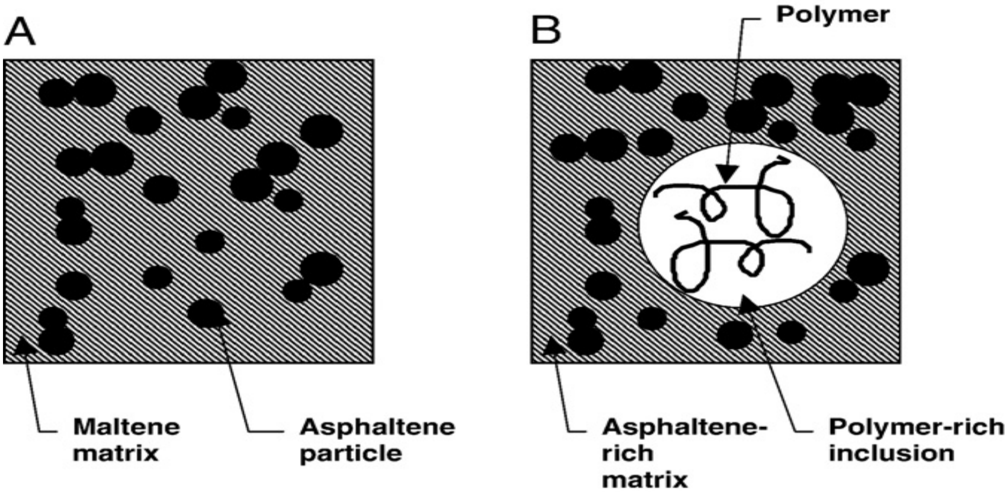

Figure 1.4 Effect of polymer-modification on the colloidal structure of a bitumen: unmodified bitumen (A) and polymer modified bitumen (B) [2].

The compatibility between SBS polymer and bitumen can be enhanced by the addition of aromatic oils or maltenes. Nevertheless, a high proportion of an aromatic content will cause the polystyrene blocks to dissolve and devastate the advantages of the SBS copolymer [18].

1.3 Fillers

Fillers which are inert and solid materials are dispersed in the bitumen matrix. They can be categorized according to its rigidity (rigid or flexible fillers), its shape (spherical, ellipsoidal, platelike or fibrous fillers) and its chemical form (organic or inorganic fillers) [23].

The general effect of adding filler to bitumen is to make it harder and stiffer [6]. On the other hand, their numerous advantages have also been realized.

Some advantages of using fillers are as follows [24]:

Reduction of cost
Improvement of process
Control of density
Thermal conductivity
Flame retandancy
Optical, electrical and magnetic properties
Mechanical properties such as hardness, stiffness, etc.

The most important factors that affect the behaviour of fillers are their particle size distribution, surface area, shape, colour, refractive index, impurities, density, hardness, moisture content, thermal stability, modulus, surface chemistry and toxicity. Particle size distribution gives information about the number of particles at a given loading, closeness of particles to each other and the size of filler surface. The compound's mechanical, physical and electrical properties depend on the volume percentage of filler. Mineral fillers have higher moduli than polymers. Additionally, particle size and shape of fillers influence the yield strength [25].

As it is observed in Figure 1.5., filler particles are covered by bitumen. Adding filler to bitumen leads to reduction in the deformation produced, and it results in an increase in softening point and stiffness and a decrease in penetration. The hardening effect depends on the amount of filler added and its particle size, shape and grading. Besides changing the rheological properties of the bitumen, the filler increases the specific gravity of the mixture due to its high density [6].

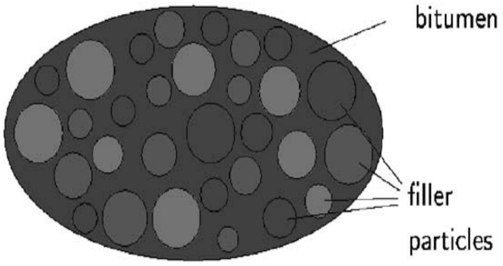

Figure 1.5 The dispersion of filler particles in bitumen [26].

1.3.1 Calcium carbonate

Calcium carbonate or calcite, which is a naturally occuring compound, is found in many rocks but it is generally related to chalk, limestone and marble [27].

Precipitated calcium carbonate can be produced in three steps:

1. Calcination: $CaCO_3 \rightarrow CaO + CO_2$
2. Hydration: $CaO + H_2O \rightarrow Ca(OH)_2$
3. Carbonation: $Ca(OH)_2 + CO_2 \rightarrow CaCO_3 + H_2O$

The process begins with the calcination of limestone at around 900°C to obtain quicklime and carbon dioxide. The quicklime is converted to the hydrated lime with water. Carbon dioxide is passed through the hydrated lime in a reactor to precipitate the desired calcium carbonate.

$CaCO_3$ is one of the most abundant and most commonly used mineral filler due to its white color, low abrasion, wide particle size ranges, and its availability and cheapness. Calcium carbonate is found in calcite and aragonite forms. Calcite is the thermodynamically stable, whereas aragonite is the metastable form of $CaCO_3$ and can be irreversibly converted to calcite by heating in dry air to 400°C [28]. ,

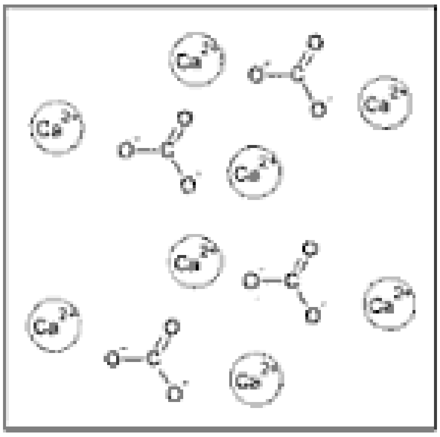

Figure 1.6 Structure of Calcium carbonate [27].

As it is seen in Figure 1.6, $CaCO_3$ can be seen as a triangle structure with Ca^{2+} cations in the center and CO_3^{2-} anions at the vertices. While carbonates lie in the same plane in the calcite form, they lie in two different planes in the aroganite form. Aroganite has a more closely packed structure, so it has higher density than calcite [27].

Table 1.2 Characteristics of Calcium carbonate ($CaCO_3$)

Chemical composition	Calcite	Aragonite
Structure	Hexagonal	Orthorhombic
Specific gravity, g/cm^3	2.71	2.93
Refractive index	1.53-1.69	1.49-1.66
Moh's hardness	3	3.5
Melting point, (^oC)	825	1339

The specific surface area of calcium carbonate is usually in the range of 2-13 m^2/g. It is directly proportional to the grain size distribution because calcium carbonate shows little porosity [29].

Calcium carbonates have been used since ancient times. The ancient Egyptians used limestone in the construction of the pyramids 5000 years ago. Now, limestone is mainly used as a construction material. It is estimated that a billion tons of crushed limestone was used in roads, dams, fill, buildings and various other construction uses in 2005 in USA [27]. Limestone is also added to roofing felt, carpet tiles, pipe enamels, clay pigeons, mastic, jointing compounds, and many other materials except where thin coatings, e.g. paints, are required [6].

1.3.2 Calcium oxide

CaO is a white caustic crystalline alkali substance. The term lime is used for calcium compounds such as quicklime (CaO) and hydrated lime ($Ca(OH)_2$).
Quicklime or CaO is produced by calcination process.

$$CaCO_{3(s)} \xrightarrow{\Delta} CaO_{(s)} + CO_{2(g)}$$

Table 1.3 Characteristics of Calcium oxide (CaO)

Chemical composition	CaO
Structure	Halite
Specific gravity, g/cm^3	3.34
Refractive index	1.83
Moh's hardness	3.5
Melting point, (^oC)	2572

The earliest use of lime is as a mortar. Also, it has been used in the production of glass since ancient times. Most modern glass produced is called soda-lime glass which consists of approximately 70 % silica, 25 % soda (Na_2O) and 5 % lime. Lime mainly is used in metallurgy, flue gas desulfurization, construction, mining, papermaking, and water treatment. Moreover, CaO serves as a drying agent by combining with water [27].

1.3.3 Manganese dioxide

Pyrolusite is the most common secondary ore of manganese. It is formed of either primary manganese minerals or the direct deposits from cold ground water. MnO_2 or pyrolusite includes manganese dioxide with a small amount of water, heavy metal, phosphorous and other metals. Its cleavage is prismatic, and it is brittle with an uneven fracture [30].

Table 1.4 Characteristics of Manganese dioxide (MnO_2)

Chemical composition	MnO_2 (pyrolusite)
Structure	Tetragonal
Specific gravity, g/cm^3	5.026
Refractive index	Opaque
Moh's hardness	6 - 6.5
Melting point, (^oC)	535

MnO_2, a dark insoluble compound, is used in glass industry, drystuff and varnish [31]. MnO_2 is also an electrochemically active component in dry cell and alkaline batteries [32].

1.3.4 Barium sulfate

Barium sulfate or baryte which is a naturally occurring mineral is obtained from rocks by leaching. It is also widespread in sedimentary rocks as concretions. It is known as barite, heavy spar, bar, tiff and baryte. Baryte is insoluble in water and acid and chemically inert. Pure baryte is white, but its color can be varied because of impurities. It has perfect cleavage, fragile with an uneven fracture [33]. In addition to its high density, $BaSO_4$ has low moisture content and pH in the range of 6-7 [29].

Table 1.5 Characteristics of Barium sulfate ($BaSO_4$)

Chemical composition	$BaSO_4$
Structure	Orthorhombic
Specific gravity, g/cm^3	4.5
Refractive index	1.64
Moh's hardness	3 - 3.5
Melting point, (^{o}C)	1580

Due to its chemical resistance, inertness and high absorptivity of light, baryte has many applications [29]. It is widely used in foams, sound insulation and floor covering [34]. Baryte mineral is also used in paving with rubber and asphalt to make roads and runways durable [33].

1.3.5 Perlite

Perlite which is a naturally occurring volcanic siliceous glass has high water content. When perlite is heated to 720-1090°C, it expands to 10-20 times its original volume, forming tiny, hollow, spherical bubbles [35]. Perlite has an amorphous aluminum silicate structure including SiO_2, Al_2O_3, K_2O, Na_2O, CaO, trace quantities of metal oxides [36].

Table 1.6 Characteristics of Perlite

Chemical composition	SiO_2, Al_2O_3, K_2O, H_2O
Structure	Amorphous
Specific gravity, g/cm^3	2.25
Refractive index	1.5
Moh’s hardness	7
Melting point, (^oC)	850

Almost all perlite is used in an expanded form, while a small amount of unexpanded perlite is consumed in a few applications. Expanded perlite is a porous and lightweight mineral [36]. Since the density of perlite is low and it is economic, it can be utilized in numerous ways (Figure 1.7).

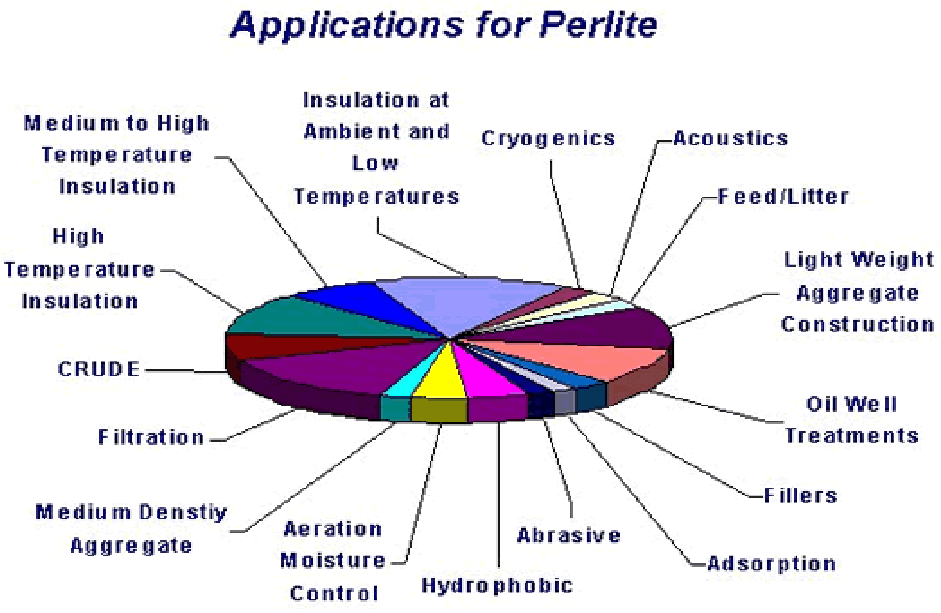

Figure 1.7 Applications of perlite.

Perlite is widely used as a heat and sound insulating material in civil engineering and as a filter medium in the chemical, food-processing, petrochemical, pharmaceutical, and aircraft industries [37]. Moreover, expanded perlite is used as an aggregate in plasters, wallboard, lightweight concrete and fire resistant coatings. It is used as cryogenic insulation in storage vessels for liquified gases, and with silicone treatment as loose fill insulation in cavities [38].

1.3.6 Vermiculite

Vermiculite, a natural occurring mineral formed of hydromica groups, expands 6-20 times of its unexpanded form when heated to about 1100°C [35]. The constitutional formula of vermiculite is $22MgO\text{-}5Al_2O_3\text{-}Fe_2O_3\text{-}22SiO_2\text{-}4H_2O$; an alternative formula is: $4.5H_2O\text{-}MgO_{0.3}\text{-}0.4(Al_2Si_6\ )(Mg,Fe,\ Al)\ 6O_{20}(OH)_4$. It crystallizes in the monoclinic system [39].

Table 1.7 Characteristics of Vermiculite

Chemical composition	MgO, Al_2O_3, Fe_2O_3, SiO_2, H_2O
Structure	Monoclinic
Specific gravity, g/cm^3	2.5
Refractive index	1.52
Moh’s hardness	1.2 - 2
Melting point, (^{o}C)	1350

As it is seen in Figure 1.8, it is a platy structure with two unit layers of silicon-oxygen tetrahedra and a layer composed of hydroxyl groups and magnesium or iron ions that form mica packets. When Si^{4+} ion is replaced by Al^{3+} ion, each packet generates a negative charge that is compensated by $Mg(6H_2O)^{2+}$ ions sandwiched between the neighbouring packets [39].

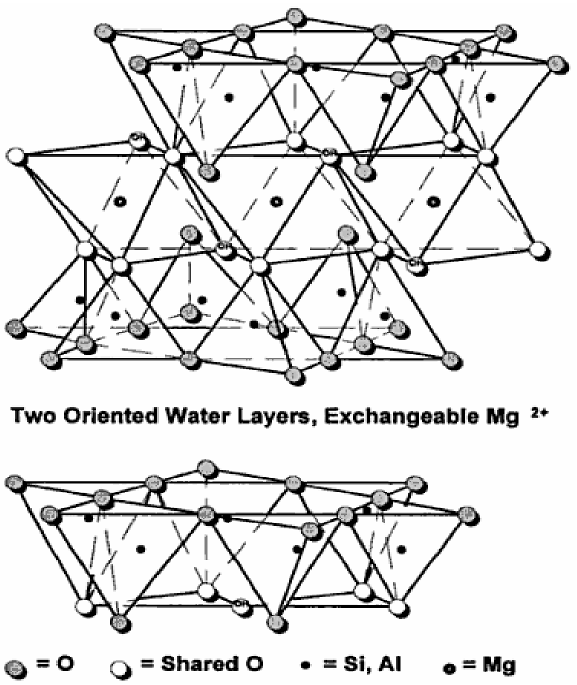

Figure 1.8 Structure of Vermiculite [40].

Vermiculite shows a good ion exchange property so it can be used to prepare materials by extracting salts of heavy metals (stronium, cesium, lead and zinc) from water. It has plate-like structure, therefore, exhibits good lubricating property over a wide temperature range [39].

The expanded vermiculite due to its unique propeties - low bulk density, low heat conductivity, relatively high melting point, chemical inertness, durability, and environmental safety- can be used as filler for thermal and sound deading applications [39]. It is also used as a density reducing filler in plastics [35].

1.4 Aim of the Study

In this study, we tried to improve the properties of bitumen-based composites. For this purpose, 20/30 and 50/70 penetration grades of bitumen were chosen. While 20/30 bitumen is more viscous and harder, 50/70 bitumen is less viscous and softer. Polymer and fillers were used as additives. SBS was used to improve the elasticity and to reduce the viscosity of composites. $CaCO_3$ and CaO were the main fillers. Other fillers, MnO_2, $BaSO_4$, perlite and vermiculite were replaced with $CaCO_3$ while the total volume fraction of the filler was kept constant in the main matrix. Characterization was carried out to determine morphological, mechanical, flowability and sound insulation characteristics of bituminous composites and to compare the effectiveness of fillers.

CHAPTER 2

EXPERIMENTAL

2.1 Materials

2.1.1 Bitumen

In this study, 20/30 and 50/70 penetration grades of bitumen were obtained from TUPRAS A.S. 20/30 bitumen is more viscous and harder, 50/70 bitumen is less viscous and softer. Some selected properties are shown in Table 2.1 and Table 2.2.

Table 2.1 Properties of 20/30 penetration grade bitumen used in the study

Property	**ASTM**	**UNIT**	**VALUE**
Penetration at 25^{o}C, 100 g, 5 s	D 5	x 0.1mm	20/30
Softening Point (ring and ball method)	D 36	^{o}C	57-67
Solubility (in dichloroethane)	D 2042	wt %	98

Table 2.2 Properties of 50/70 penetration grade bitumen used in the study

Property	**ASTM**	**UNIT**	**VALUE**
Penetration at 25^{o}C, 100 g, 5 s	D 5	x 0.1mm	50/70
Softening Point (ring and ball method)	D 36	^{o}C	46-54
Solubility (in dichloroethane)	D 2042	wt %	99

2.1.2 SBS

SBS block copolymer was supplied by Elastron Kimya A.S. Some selected properties of SBS are shown in Table 2.3.

Table 2.3 Properties of SBS used in this study

Property	**ASTM**	**UNIT**	**VALUE**
Hardness	ASTM D-2240	Shore A	70 ± 2
Density	ASTM D-792	g/cm^3	1.03 ± 0.02
Tensile strength at break	ASTM D-412	kgf/cm^2	65 ± 7
Elongation at break	ASTM D-412	%	750 ± 100
Tear resistance	ASTM D-624	N/mm	50

2.1.3 Fillers

2.1.3.1 Calcium carbonate

$CaCO_3$ used in this study was obtained from OMYA Madencilik A.Ş. Its specific gravity is 2.71 g/cm^3 and it is a precipitated $CaCO_3$. The chemical composition of $CaCO_3$ is shown in Table 2.4.

Table 2.4 Chemical composition of Calcium carbonate

Material	**Composition (%)**
$CaCO_3$	98.5
$MgCO_3$	1.5
Fe_2O_3	0.05

2.1.3.2 Calcium oxide

CaO was supplied by J.T. Baker. Molecular weight is 56.08 g/mol. Its specific gravity is 3.34 g/cm^3. The relevant composition of CaO is shown in Table 2.5.

Table 2.5 Chemical composition of Calcium oxide

Material	Composition (%)
CaO	94.0
MgO	0.4
CO_2	2.0
SiO_2	0.8
Fe_2O_3	0.2
Al_2O_3	0.3
SO_3	0.2

2.1.3.3 Manganese dioxide (or Mangan (IV) oxide)

MnO_2, the product of Riedel-de Haen, has molecular weight 86.94 g/mol. Its specific gravity is 5.026 g/cm^3. MnO_2 or pyrolusite includes manganese dioxide with a small amount of water, heavy metal, phosphorous and other metals.

2.1.3.4 Barium sulfate

$BaSO_4$ was obtained from Baser Mining Ind. & Com. Inc. Molecular weight is 233.43 g/mol. Its specific gravity is 4.5 g/cm^3. The chemical composition of $BaSO_4$ is shown in Table 2.6.

Table 2.6 Chemical composition of Barium sulfate

Material	Composition (%)
$BaSO_4$	98
SiO_2	1.2
Fe_2O_3	0.05

2.1.3.5 Perlite

Perlite was supplied by Eti Maden İşletmeleri. Its specific gravity is 2.25 g/cm^3. The chemical composition of perlite is shown in Table 2.7.

Table 2.7 Chemical composition of Perlite

Material	Composition (%)
SiO_2	70-75
Al_2O_3	12-15
Na_2O	3-4
K_2O	3-5
Fe_2O_3	0.5-2
MgO	0.2-0.7
CaO	0.5-1.5
Chemical/combined water	3-5

2.1.3.6 Vermiculite

Vermiculite was recovered from packing box. Its specific gravity is 2.5 g/cm^3. The chemical composition of vermiculite is shown in Table 2.8.

Table 2.8 Chemical composition of Vermiculite

Mineral	Composition (%)
SiO_2	38-46
Al_2O_3	10-16
MgO	16-35
CaO	1-5
K_2O	1-6
Fe_2O_3	6-13
TiO_2	1-3
H_2O	8-16
Other	0.2-1.2

2.2 Sample Preparation

Blends were prepared on the basis of the volume percentage of materials. The volume percentages of bitumen, SBS and CaO were kept constant (Table 2.9) while volume fractions of $CaCO_3$ and other fillers were changed. As the amount of $CaCO_3$ was decreased, other main fillers were added in the ratios given in Table 2.10. As it is seen in the Table 2.10, the volume percentages of MnO_2 and perlite could not be higher than 7 % because it was not possible to process the composites above that percentage at 130°C. However, this ratio could be increased for $BaSO_4$ and vermiculite.

Table 2.9 Volume percentages of constants in the bituminous composites.

Bitumen 20/30 %	Bitumen 50/70 %	SBS %	CaO %
19	22	2	2

Table 2.10 Volume percentages of fillers in the bituminous composites.

Composite	$CaCO_3$ %	MnO_2 %	$BaSO_4$ %	Perlite %	Vermiculite %
55% $CaCO_3$	55				
3% MnO_2	52	3			
5% MnO_2	50	5			
7% MnO_2	48	7			
3% $BaSO_4$	52		3		
5% $BaSO_4$	50		5		
7% $BaSO_4$	48		7		
15% $BaSO_4$	40		15		
20% $BaSO_4$	35		20		
30% $BaSO_4$	25		30		
40% $BaSO_4$	15		40		
50% $BaSO_4$	5		50		
3% Perlite	52			3	
5% Perlite	50			5	
7% Perlite	48			7	
3% Vermiculite	52				3
5% Vermiculite	50				5
7% Vermiculite	48				7
15% Vermiculite	40				15
20% Vermiculite	35				20
30% Vermiculite	25				30

2.2.1 Mixing

The composites were prepared in a Brabender Plasti-Coder Torque Rheometer model PLV 151 (Figure 2.1) at a temperature of 130^{o}C. The capacity of Brabender is 50 ml. Materials were added in the order of bitumen, polymer and fillers. After the addition of bitumen, polymer was added. They were mixed for 5 minutes, and then the fillers were added. Each experiment was carried out at 60 rpm by mixing the materials for 20 minutes.

Figure 2.1 Brabender Plasti-Coder Torque Rheometer model PLV 151

The mixing chamber was heated by circulating oil and a thermometer was used to monitor the oil temperature.

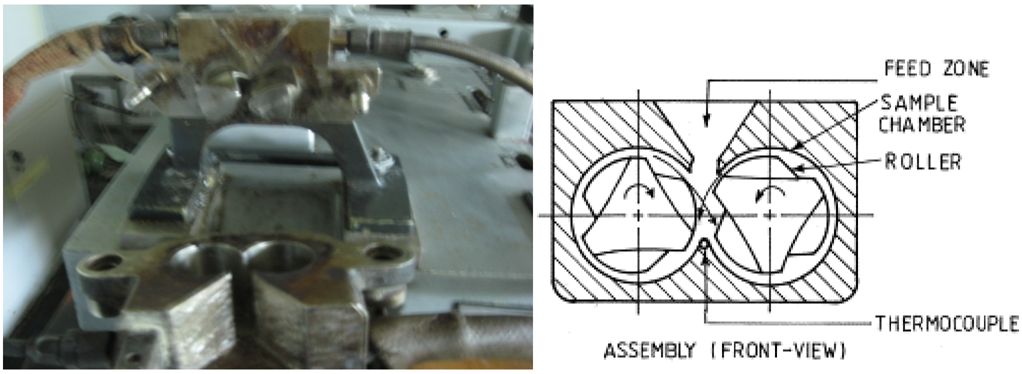

Figure 2.2 Schematic diagram of an internal roller mixer

As it is seen in Figure 2.2, it has two rollers which counter rotate for better mixing.

2.2.2 Compression Molding

The composites that were prepared in Brabender were molded using Hot-press machine (Figure 2.3) at 130°C. PET overhead transparencies were used for easy removal of composites from the steel molds. The mold was closed and placed between two heated platens of the compression molding equipment. A slight pressure was applied until the material melted. Then, molded blends were cooled at room temperature at the normal atmospheric pressure.

Figure 2.3 Hot-Press Machine

2.3 Characterization

2.3.1 Particle Size Analysis of Fillers

The Mastersizer 2000 is designed for the particle size distribution measurements of wet and dry samples. It has a wide range of sample dispersion units including an autosampler. Due to its range of detector angles covering forward scattering, wide angle forward scattering, side scattering, and back scattering, and the use of two different wavelengths of incident light, the accessible particle size ranges from 0.02 μm to 2000 μm [41].

Figure 2.4 Particle Size Analyzer (Malvern Mastersizer 2000)

Since properties of many materials such as stability, reactivity, opacity, flow characteristics etc. are affected by the size and the characteristics of the particles within, the particle size measurement is important. The particle size distributions of fillers used in this study were determined using Mastersizer 2000, Malvern Instruments at METU Central Research Laboratory (Figure 2.4). 200 mg of each sample was used in determining the particle sizes of fillers by using wet method.

2.3.2 Morphological Analysis

2.3.2.1 Scanning Electron Microscopy

The Scanning Electron Microscopy (SEM) forms an image of the surface contours of a specimen [42]. The term “scanning” in the context of Scanning Electron Microscopy is used to describe the method of producing the magnified image. A focused electron beam or probe scans the specimen surface, while the image is formed on the screen of synchronously scanned cathode ray tube. The magnification is expressed as the ratio of lengths of the two rasters. In the scanning microscope, each point on the screen represents a point on the specimen.

Figure 2.5 Scanning Electron Microscopy (QUANTA 400F Field Emission)

In this study, SEM at METU Central Research Laboratory (Figure 2.5) was used to analyze the morphologies of bituminous composites. The fracture surfaces of blends were characterized. The images were magnified x500 and x2500.

2.3.3 Density Measurements

Density measurements were done by using electronic densimeter manufactured by Alfa Mirage Co. Ltd at room temperature.

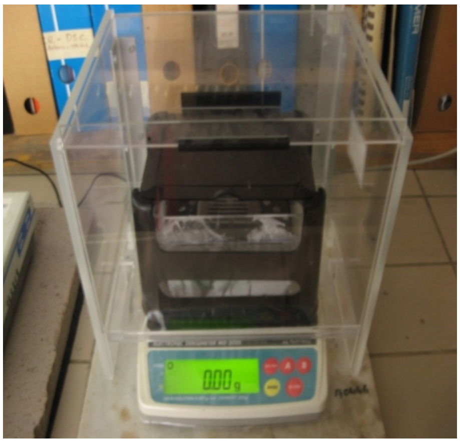

Figure 2.6 Electronic Densimeter (Alfa Mirage MD-300S)

2.3.4 Mechanical Analysis

2.3.4.1 Tensile Test

Mechanical characterization of the bituminous composites was done by using tensile test machine at room temperature. Tensile tests were performed according to ASTM D 638-M 91a by using a Lloyd LR 5K Computer Controlled Tensile Test Machine (Figure 2.7). The speed of test was 10 cm/min.

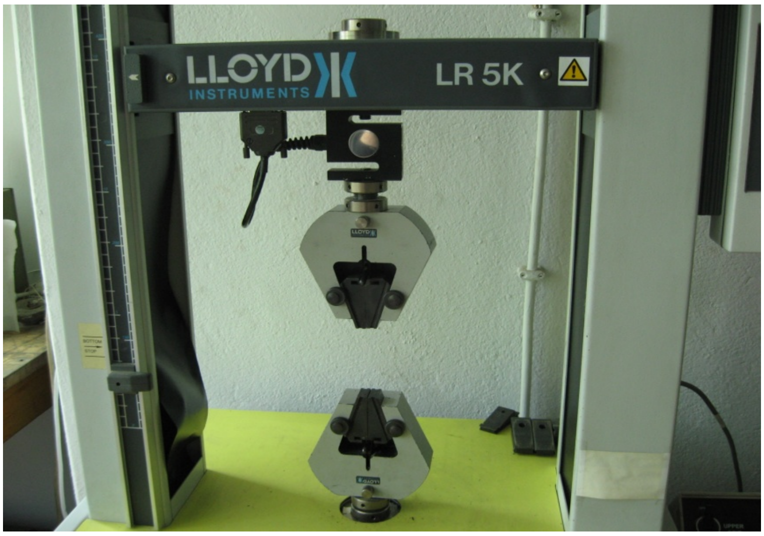

Figure 2.7 Tensile Test Machine (Lloyd LR 5K)

Tensile tests were performed on dog bone shaped molded samples. The shape of ASTM tensile test specimen is seen in Figure 2.8.

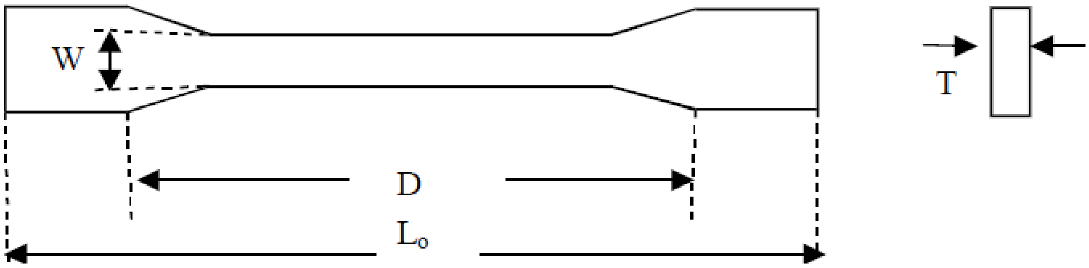

Figure 2.8 ASTM Tensile Test Specimen

The dimensions of tensile test specimen in this study are given in Table 2.11.

Table 2.11 Tensile test specimen dimensions

Symbol	Specimen Dimension
W, Width of narrow section	12
D, Distance between grips	90
L_0, Total length of specimen	140
T, Thickness of specimen	2.5

2.3.5 Flow Characteristics

2.3.5.1 Melt Flow Index (MFI)

The Melt Flow Index (MFI) is defined as the weight of the material extruded in 10 minutes through a capillary of specific diameter and length by pressure applied through dead weight under prescribed temperature conditions (Figure 2.9) [43].

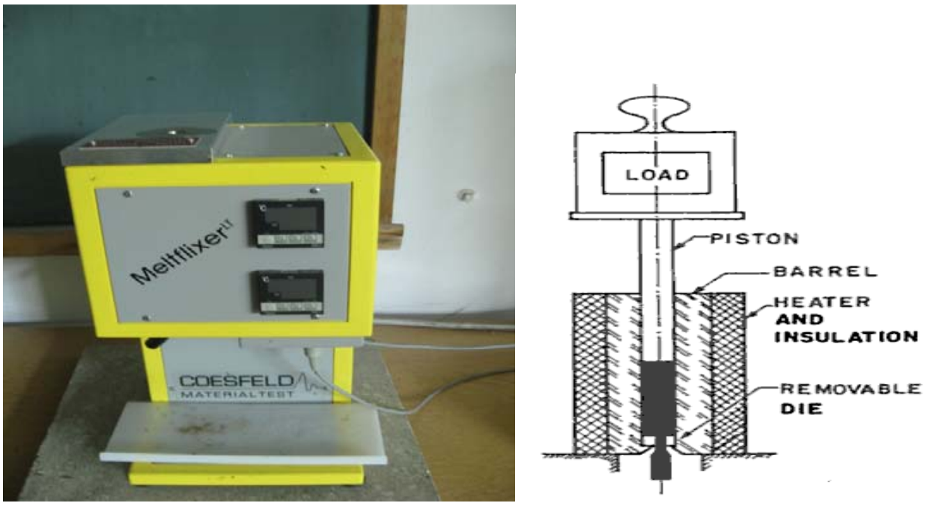

Figure 2.9 Melt Flow Index

Melt Flow Index (MFI) was performed in order to determine the flow behavior of the samples, which is inversely related to melt viscosity. The MFI values gave the effect of fillers on the rheological characteristics of the materials. Coesfield Material Test, Meltfixer LT (Figure) was used for the test. The measurements were done at three temperatures of 130 °C, 150°C and 180°C. Materials were allowed to melt in the Meltflixer for 5 minutes. Then standard weight was placed on the piston of the instrument to compress the sample. After that, the weight of the flow sample was recorded in grams/10 min (g/10min). The test was carried out under two specified loads of 2.16 kg and 5 kg.

2.3.6 Sound Insulation Characteristics

2.3.6.1 Oberst Test

According to Oberst beam technique, the material to be tested lays on a metal beam and from the vibration parameters of the metal and the composite beams, it is possible to define the properties of the viscoelastic material [44].

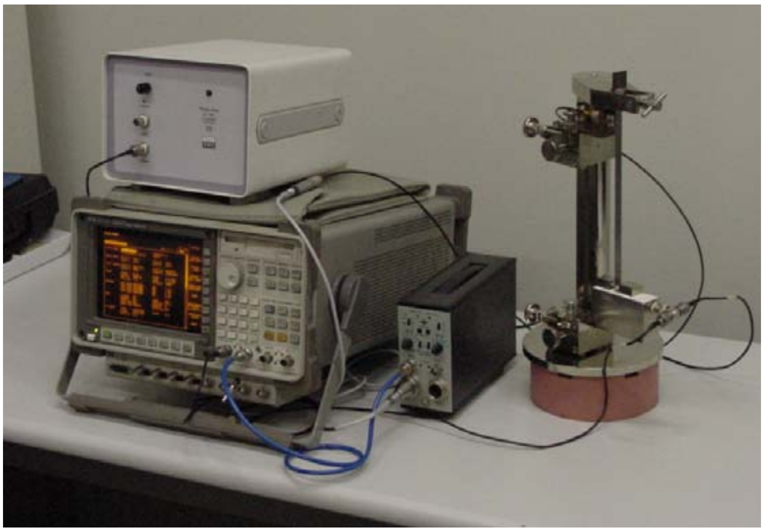

Figure 2.10 Oberst Test Machine

Oberst Test Machine at ARÇELİK ArGe Vibration Acoustics Laboratory (Figure 2.10) was used to determine the sound insulation properties of bituminous composites. It gives information about the damping ratio of composites in different frequencies at 3 different temperatures (20°C, 40°C and 60°C).

CHAPTER 3

RESULTS AND DISCUSSION

3.1 Particle Size Analysis of Fillers

Analyses of particle sizes were performed in Mastersizer 2000. The results of the test are given in Table 3.1 below.

Table 3.1 Average particle size analysis of fillers

Fillers	Average particle size (μm)
$CaCO_3$	6.9
CaO	36
MnO_2	7.5
$BaSO_4$	7.7
Perlite	28.1
Vermiculite	48.3

* The particle size of CaO is given by the producer company otherwise you cannot do this measurement in water. Particle size distribution histograms are given in Appendix B.

Particle size analysis shows that all fillers are in micron size, and it can be seen in SEM images that they were all mixed well. Although CaO has higher particle size, it has ability to hold moisture and provides a better mixing with bitumen. It is converted to $Ca(OH)_2$ because of humidity and $Ca(OH)_2$ can also interact with bitumen. Above 7% MnO_2 in composites, it was observed that the mixing process of materials was difficult. It may be because of aggregation. $BaSO_4$, on the other hand, is similar to $CaCO_3$ in terms of size and structure. Therefore, $BaSO_4$ can easily replace $CaCO_3$ and both are well mixed. Perlite is hard due to its glassy structure (degree of hardness is about 7) and increase in perlite concentration in composites makes bitumen brittle. The mixing process of vermiculite composites is easier than

MnO_2 and perlite because of its porosity and softness (degree of hardness is about 1.2-2). However, the vermiculite content could not be reached above 30% in the blending process due to its larger size and flake-like structure.

3.2 Morphological Analysis

3.2.1 Scanning Electron Microscopy

Scanning Electron Microscopy was performed to observe the effect of fillers on the bitumen morphology. The tensile fractured surfaces of bituminous composites were characterized by microscopy. The SEM images are presented with the magnifications of x500 and x2500.

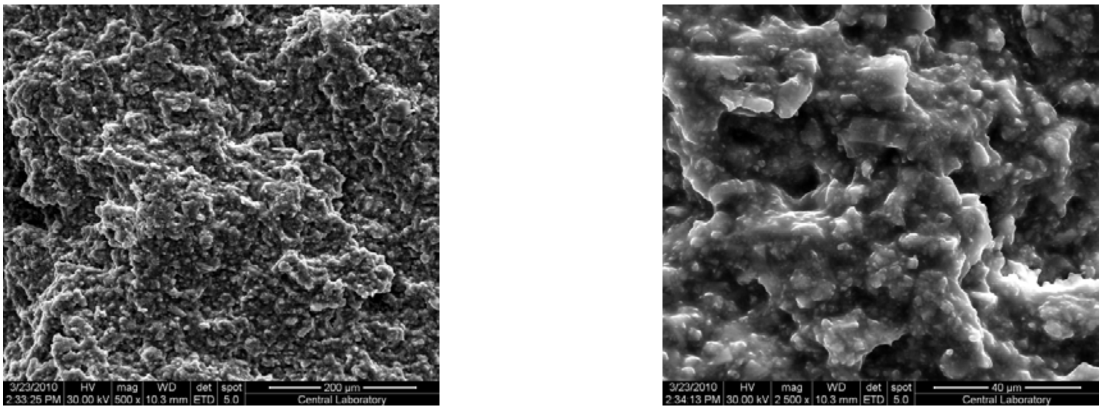

Figure 3.1 SEM micrographs of bituminous composite containing 55% $CaCO_3$ at a) x500 and b) x2500 magnifications

As it is seen in Figure 3.1 above, $CaCO_3$ particles were covered by bitumen forming a continuous phase. The following figures represent the mixtures of MnO_2, $BaSO_4$, perlite and vermiculite. No significant difference between the SEM images of composites was observed except for those of vermiculite composites.

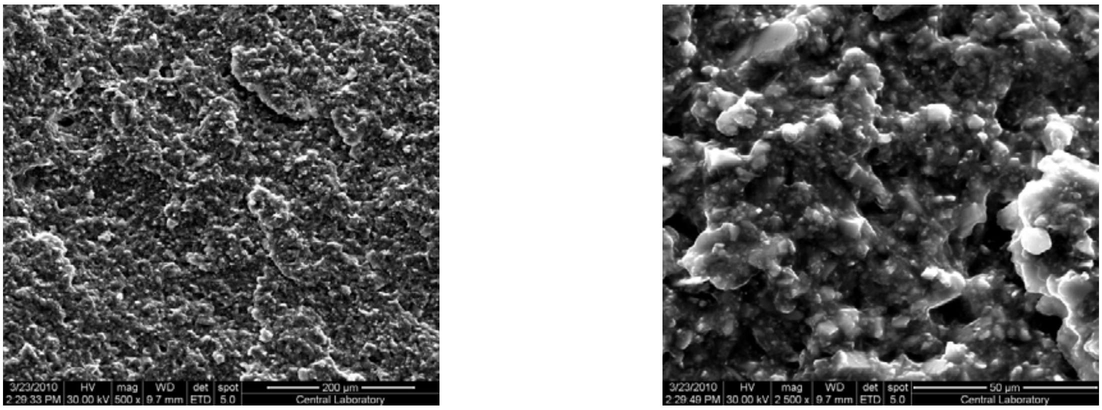

Figure 3.2 SEM micrographs of bituminous composite containing 3% MnO_2 at a) x500 and b) x2500 magnifications

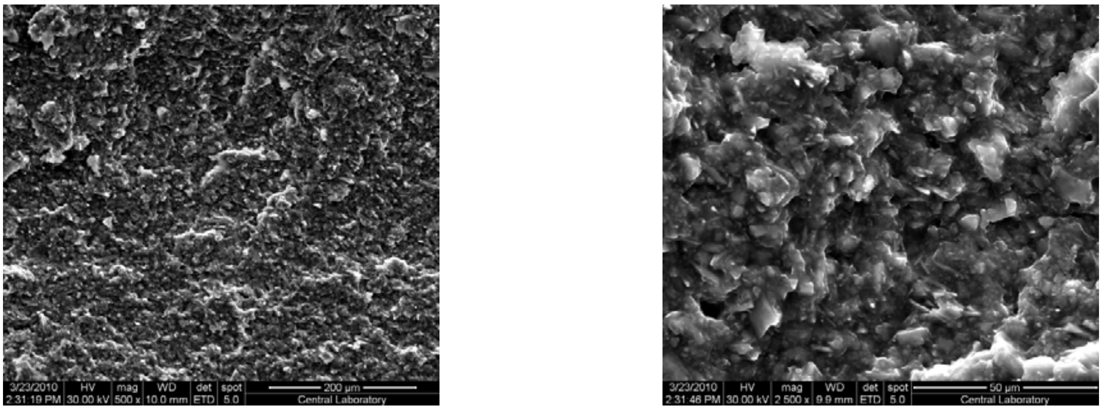

Figure 3.3 SEM micrographs of bituminous composite containing 7% MnO_2 at a) x500 and b) x2500 magnifications

SEM micrographs of MnO_2 composites show that MnO_2 particles were surrounded by bitumen and a homogeneous mixture was formed. As it is seen in Figure 3.3, when MnO_2 concentration increased in the composite, different shapes, like micron size rods, were formed. These structures may have been observed because of the irregular shape or various crystal phase of MnO_2 particle.

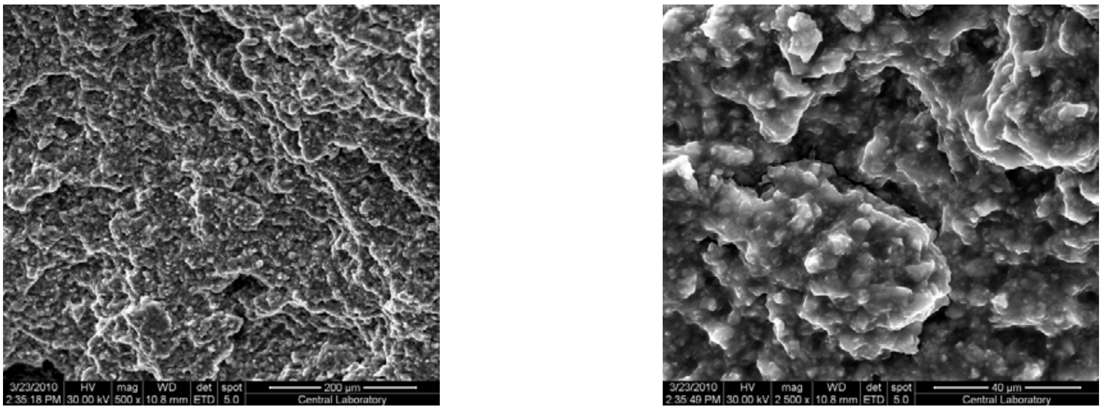

Figure 3.4 SEM micrographs of bituminous composite containing 3% $BaSO_4$ at a) x500 and b) x2500 magnifications

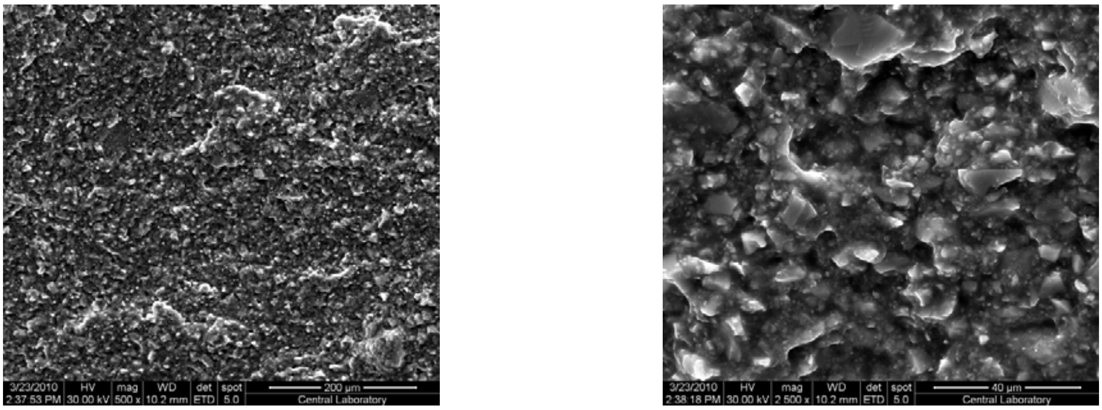

Figure 3.5 SEM micrographs of bituminous composite containing 7% $BaSO_4$ at a) x500 and b) x2500 magnifications

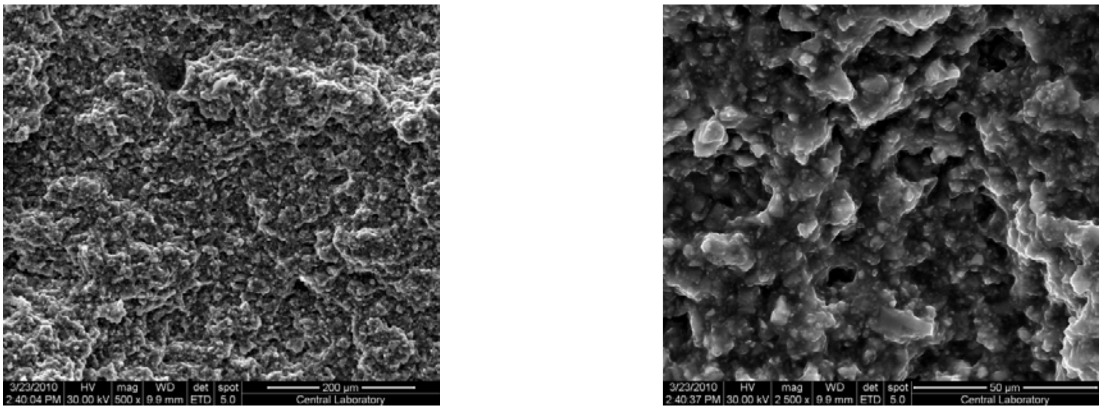

Figure 3.6 SEM micrographs of bituminous composite containing 15% $BaSO_4$ at a) x500 and b) x2500 magnifications

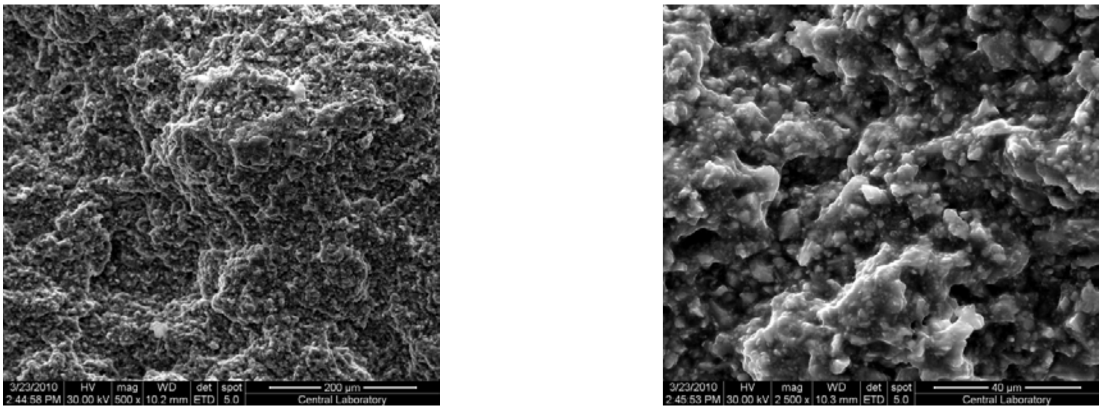

Figure 3.7 SEM micrographs of bituminous composite containing 40% $BaSO_4$ at a) x500 and b) x2500 magnifications

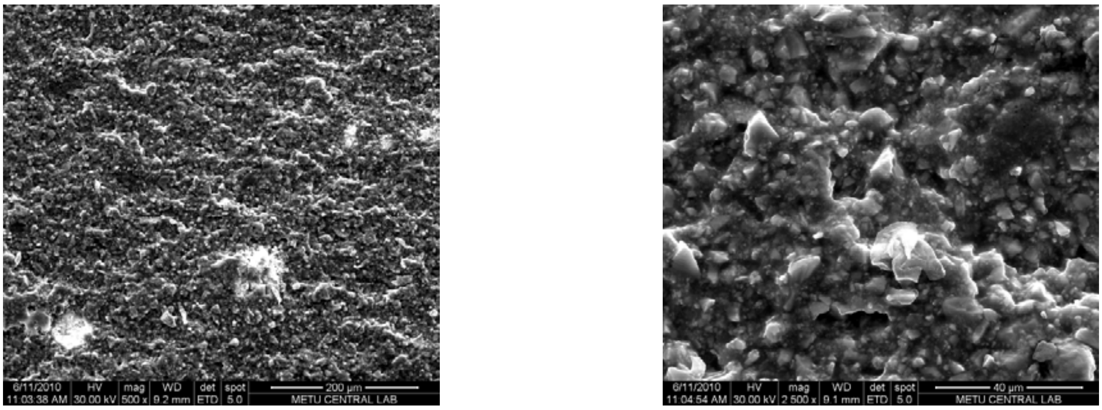

Figure 3.8 SEM micrographs of bituminous composite containing 50% $BaSO_4$ at a) x500 and b) x2500 magnifications

It is observed that $BaSO_4$ particles were well dispersed in bitumen like $CaCO_3$. $BaSO_4$ molecule is similar to $CaCO_3$ in terms of size and structure, therefore, SEM images of $BaSO_4$ particles are similar to those of $CaCO_3$. Although $BaSO_4$ content in the composites was increased to 50%, homogeneous mixture was obtained. Some bright parts of Figure 3.8 indicate the agglomeration of $CaCO_3$.

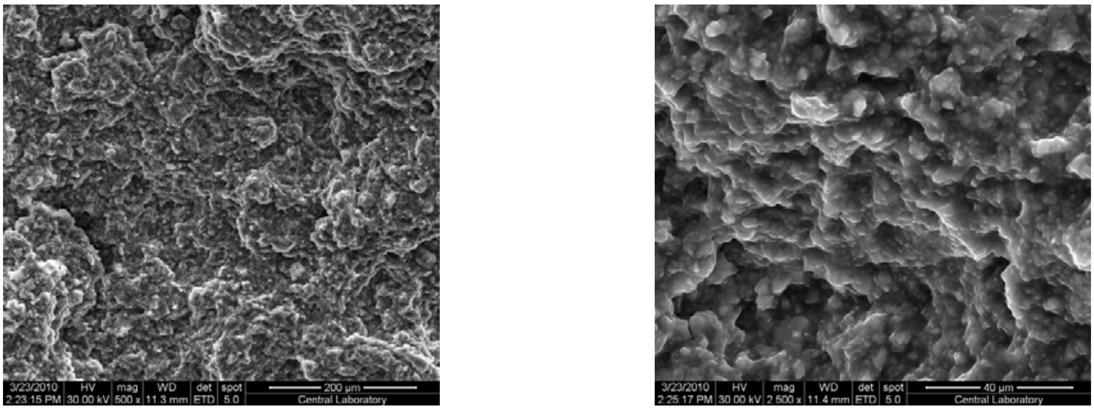

Figure 3.9 SEM micrographs of bituminous composite containing 3% Perlite at a) x500 and b) x2500 magnifications

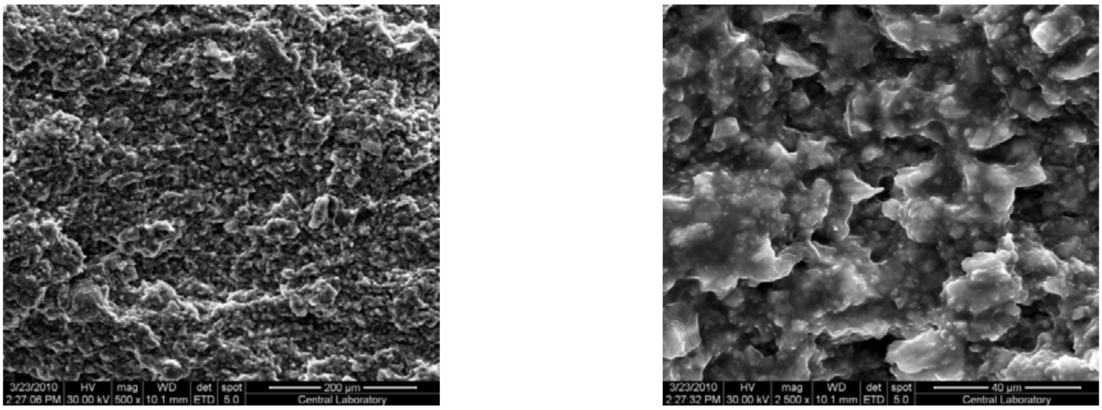

Figure 3.10 SEM micrographs of bituminous composite containing 7% Perlite at a) x500 and b) x2500 magnifications

Expanded perlite has some oil adsorption capacity due to its high porosity compared to others. It can adsorb the oil fractions or maltenes of bitumen. This property, though not very clearly, can be observed in Figure 3.10. If the amounts of bitumen and perlite in the blend were higher while that of $CaCO_3$ was low, the adsorption of oil fractions could have been seen clearly. However, the volume fractions of bitumen, SBS and CaO were kept constant in this study.

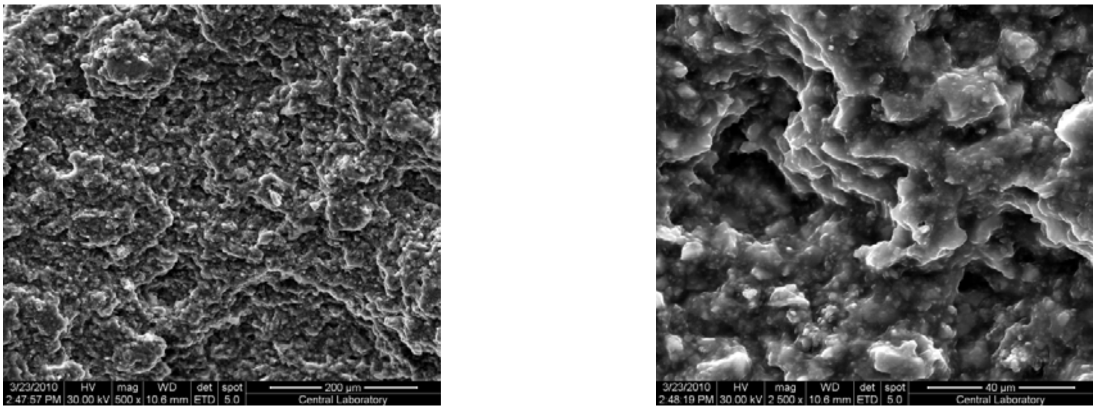

Figure 3.11 SEM micrographs of bituminous composite containing 3% Vermiculite at a) x500 and b) x2500 magnifications

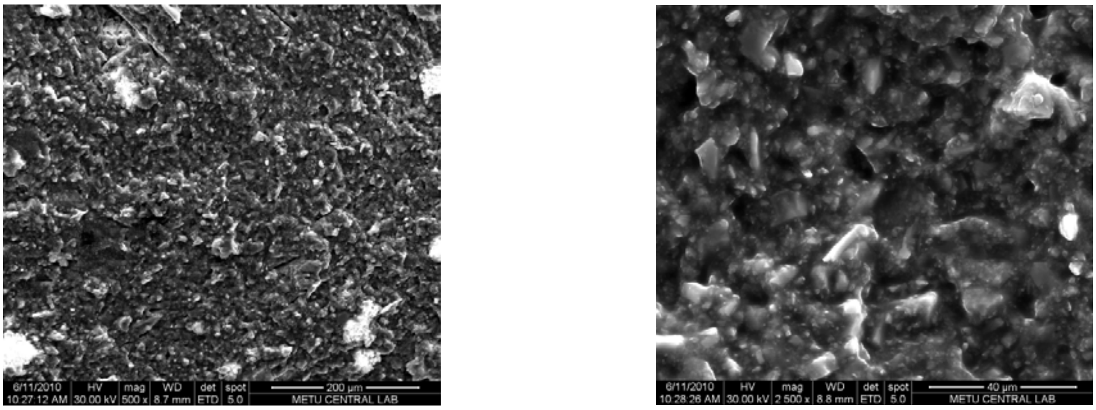

Figure 3.12 SEM micrographs of bituminous composite containing 7% Vermiculite at a) x500 and b) x2500 magnifications

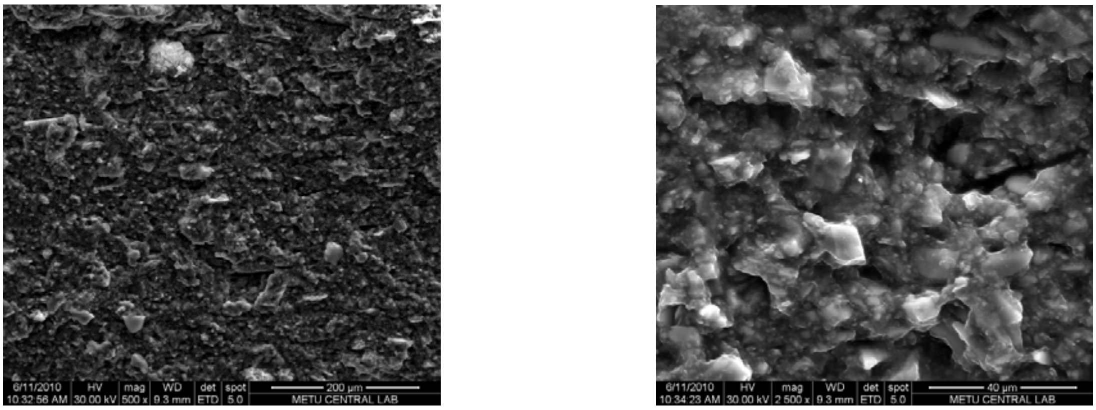

Figure 3.13 SEM micrographs of bituminous composite containing 15% Vermiculite at a) x500 and b) x2500 magnifications

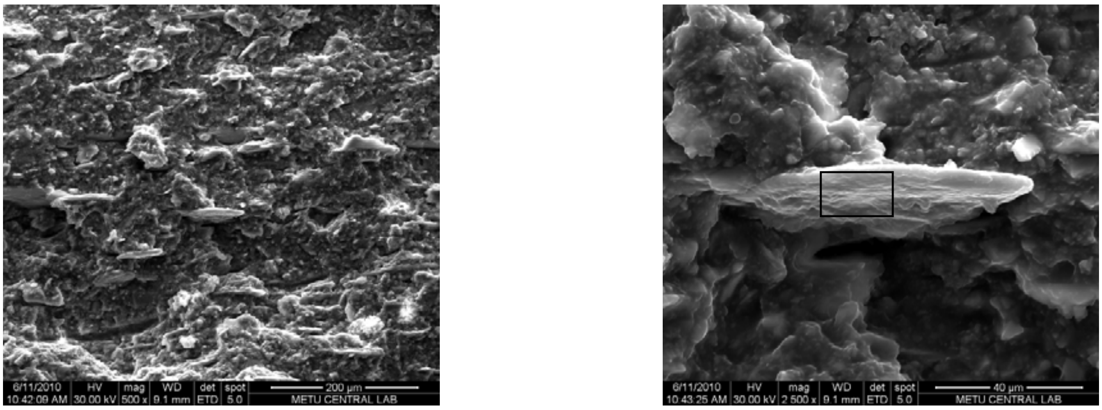

Figure 3.14 SEM micrographs of bituminous composite containing 20% Vermiculite at a) x500 and b) x2500 magnifications

Flat or platy shapes were observed in SEM micrographs of vermiculite composites because of its plate-like structure. When the amount of vermiculite in the mixtures was increased, more flat shapes were observed. These flat shapes were analyzed by EDX in SEM for 20% vermiculite composite in Figure 3.14b (the rectangle area). Figure 3.15 shows the elements found in the point specified in Figure 3.14b.

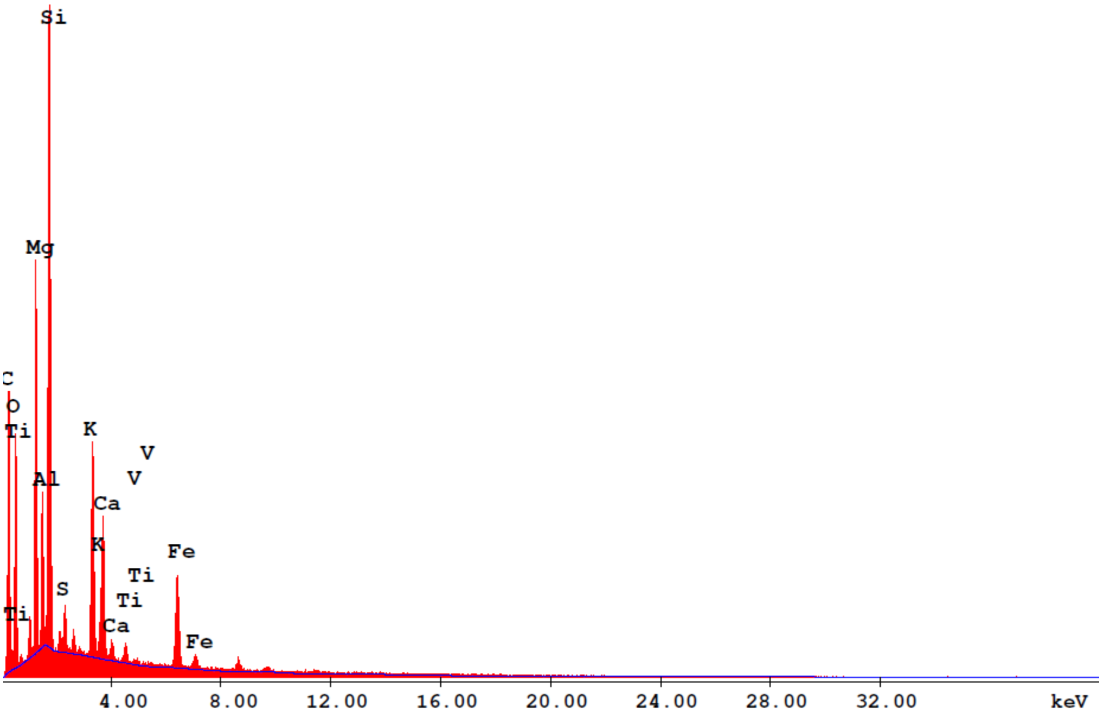

Figure 3.15 SEM-EDX Element analysis of 20% Vermiculite composite

According to Figure 3.15, Si, Al, Mg, Ca, K, Fe, Ti, C, O elements confirm the presence of vermiculite since vermiculite composite includes SiO_2, Al_2O_3, MgO, CaO, K_2O, Fe_2O_3, TiO_2 and others.

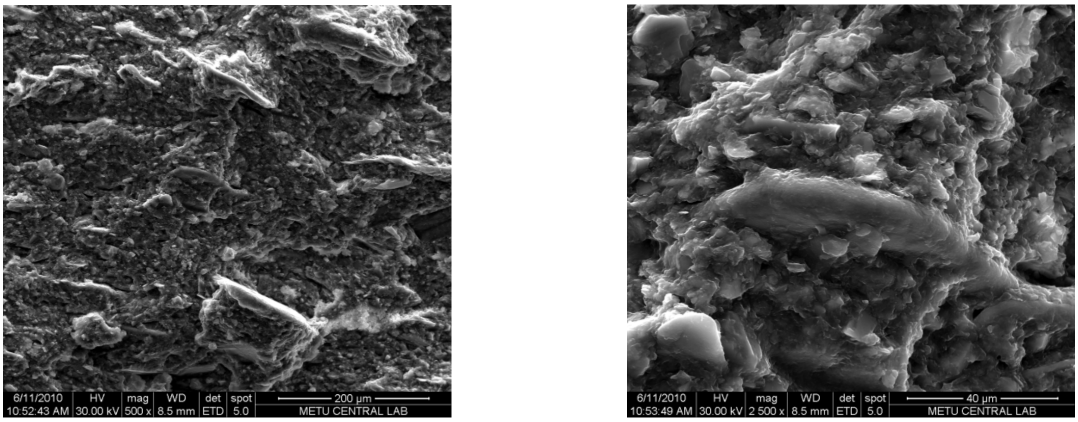

Figure 3.16 SEM micrographs of bituminous composite containing 30% Vermiculite at a) x500 and b) x2500 magnifications

3.3 Density Measurements

The existence of voids and bubbles in the composites can be determined by comparing the experimental and calculated densities of the specimens. The deviation from calculated density is an indicator of void volume in the structure of bituminous composite. Experimental densities are obtained from the densitometer. In the figures, 0 point indicates the density of 55% $CaCO_3$ composite. The other numbers such as 3, 5, 7 etc. represent the volume percentage of filler compositions.

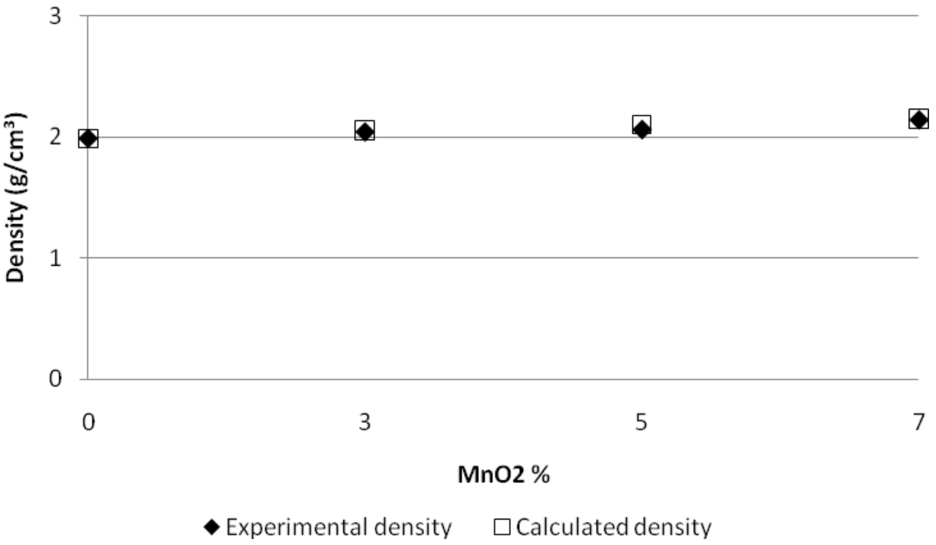
3
2
1
0
Density (g/cm³)
0
3
5
7
MnO2 %
◆ Experimental density
☐ Calculated density

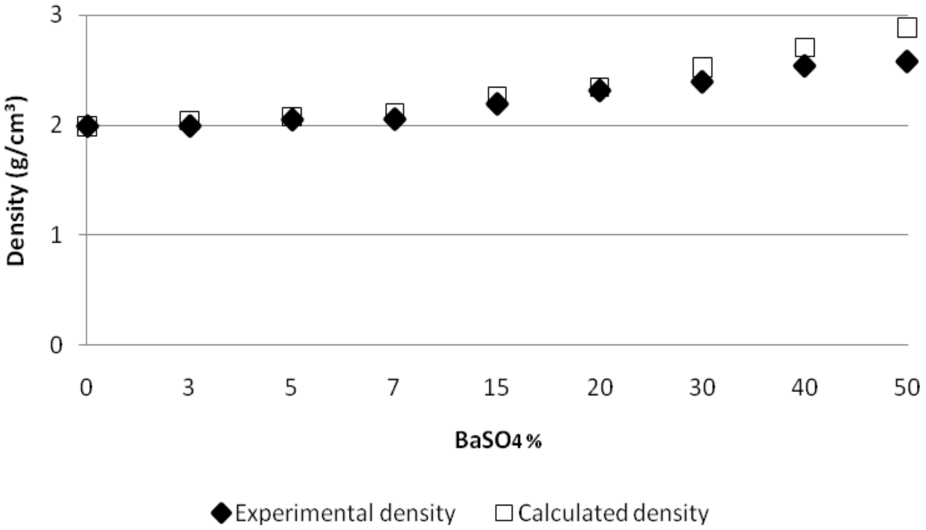
3
2
1
0
Density (g/cm³)
0
3
5
7
15
20
30
40
50
BaSO4 %
◆ Experimental density
☐ Calculated density

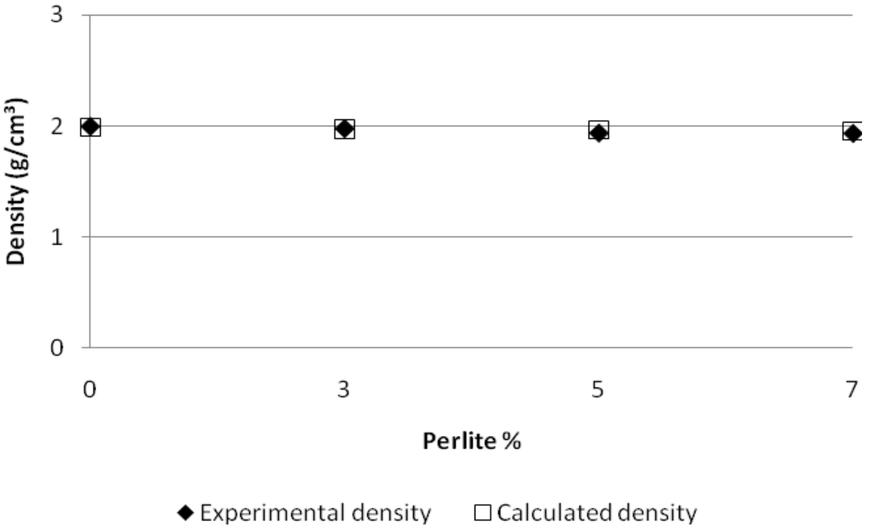
3
2
1
0
Density (g/cm³)
0
3
5
7
Perlite %
◆ Experimental density
☐ Calculated density

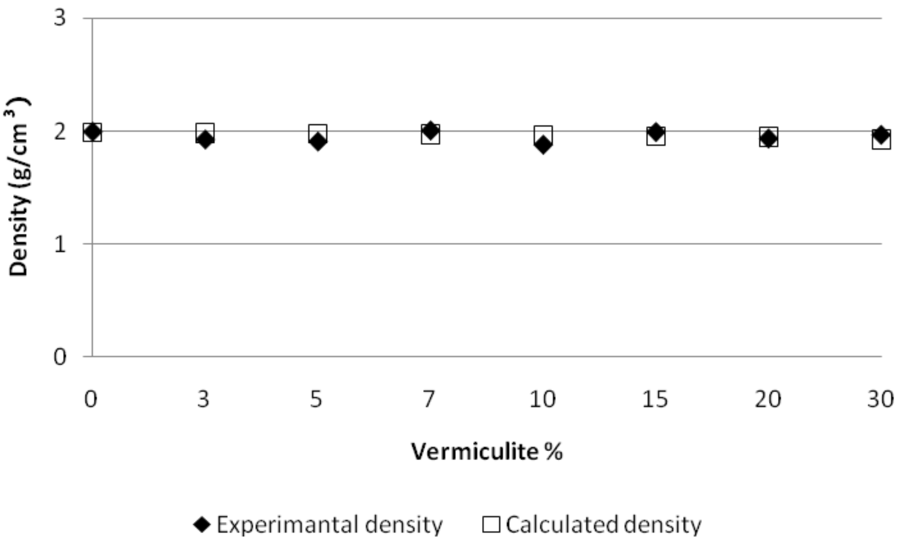

Figure 3.17 The comparison of experimental and calculated densities of bituminous composites

The closeness of the values between the experimental and calculated densities shows how well the fillers and bitumen in composites have interacted. The small density differences in $BaSO_4$ composites appear because of the possible void volumes formed while the composites were molded into plates. However, this small density differences could not be observed in SEM photos of $BaSO_4$ composite.

3.4 Mechanical Analysis

3.4.1 Tensile Test

Tensile test was performed in order to determine the effects of fillers and filler concentrations on the mechanical properties of the bituminous composites. Stress-strain at break values of composites obtained from tensile test results provide information about the response of the composites to applied stress during the test. Figures below represent the stress-percentage strain at break values of composites comparing with $CaCO_3$ composite at break values. All figures show that the addition of mineral matters by reducing $CaCO_3$ improves the mechanical properties of the bituminous composite. $CaCO_3$ composite has high percentage strain, however, low stress at break values. The composites including MnO_2, $BaSO_4$, perlite, vermiculite as fillers have higher stress at break values. The specimens that have percentage strain higher than 6 % and stress higher than 3 MPa at break values give better results in application areas.

The following figures were drawn similarly. Each data point represents the corresponding composition of the fillers given for the stress and strain at break.

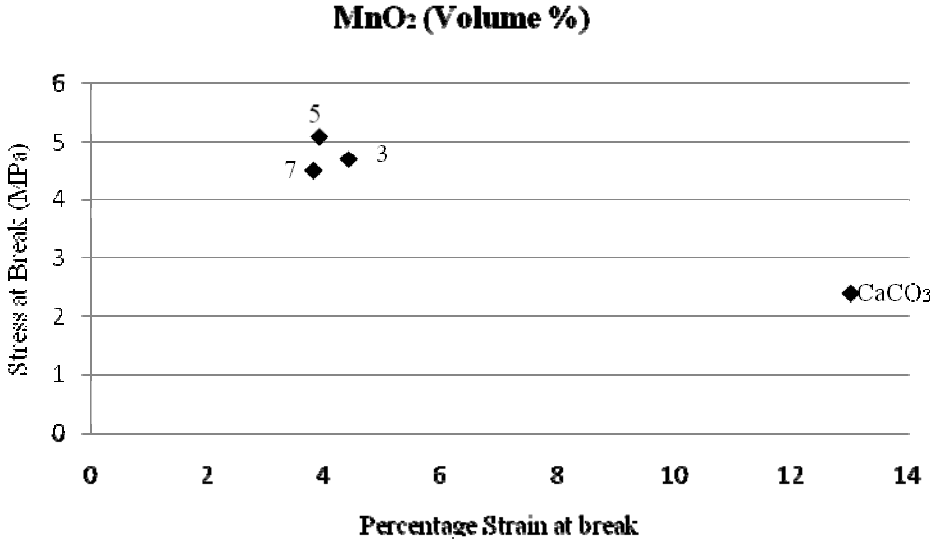

Figure 3.18 Stress- strain at break values of 3, 5 and 7% MnO_2 composites

Figure 3.18 above shows that while MnO_2 composites have high tensile strength, they have low percentage strain at break. Obtaining high stress value in MnO_2 composites is important, however the molded composites should also stretch without breaking. For this reason, MnO_2 composites cannot be appropriate for implementations because it shows very fragile characteristic. MnO_2 addition could not be done above 7% since MnO_2 composites crumbled and the composites were not homogeneous.

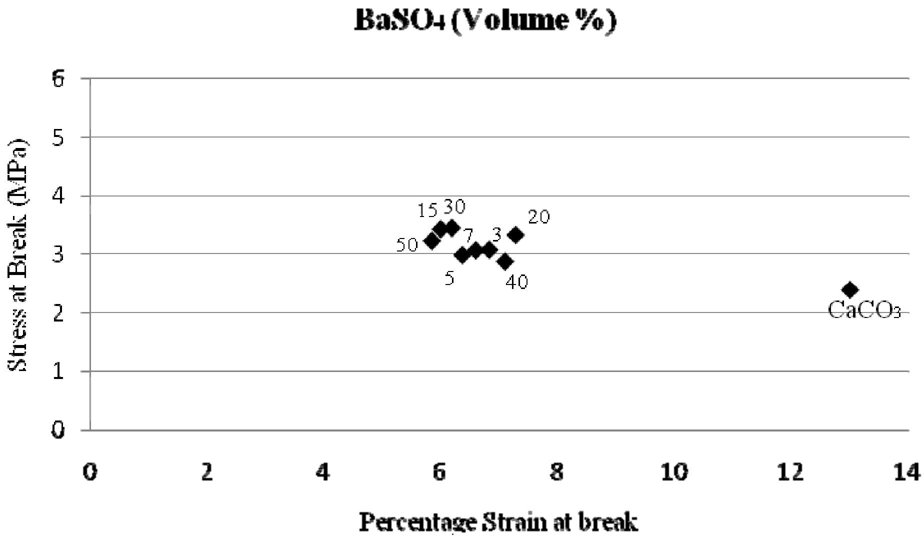

Figure 3.19 Stress- strain at break values of 3, 5, 7, 15, 20, 30, 40 and 50% $BaSO_4$ composites

All $BaSO_4$ composites gave better results for both stress at break values and percentage strain values. As it is observed in Figure 3.19, increase in $BaSO_4$ content in composites did not cause a significant change in mechanical properties. All $BaSO_4$ composites have tensile strength values between 3 and 3.5 MPa and percentage strain values between 6 and 8 %.

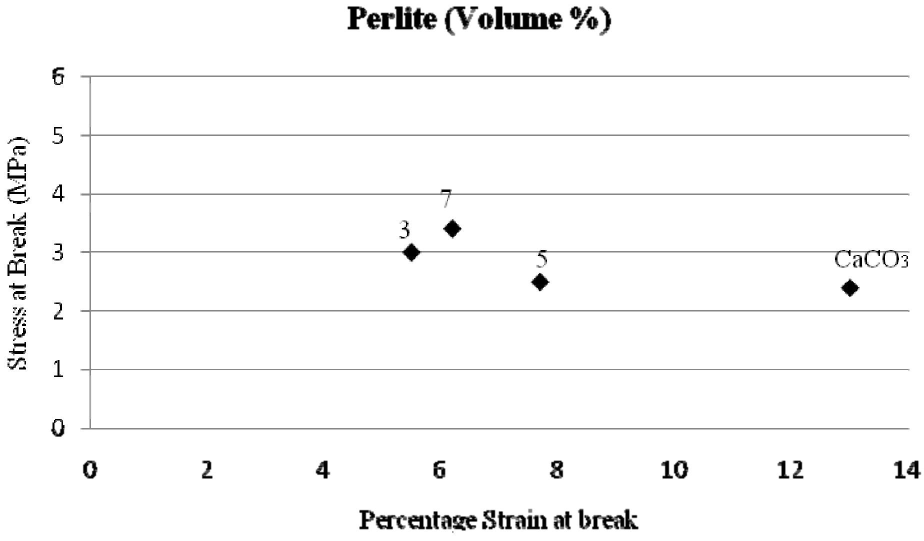

Figure 3.20 Stress- strain at break values of 3, 5 and 7% Perlite composites

Figure 3.20 indicates that 3% and 7% perlite composites have good mechanical properties. However, problems encountered with MnO_2 composites were also observed above 7% perlite. Perlite composites could not be prepared above this ratio because they were crumbled during the mixing.

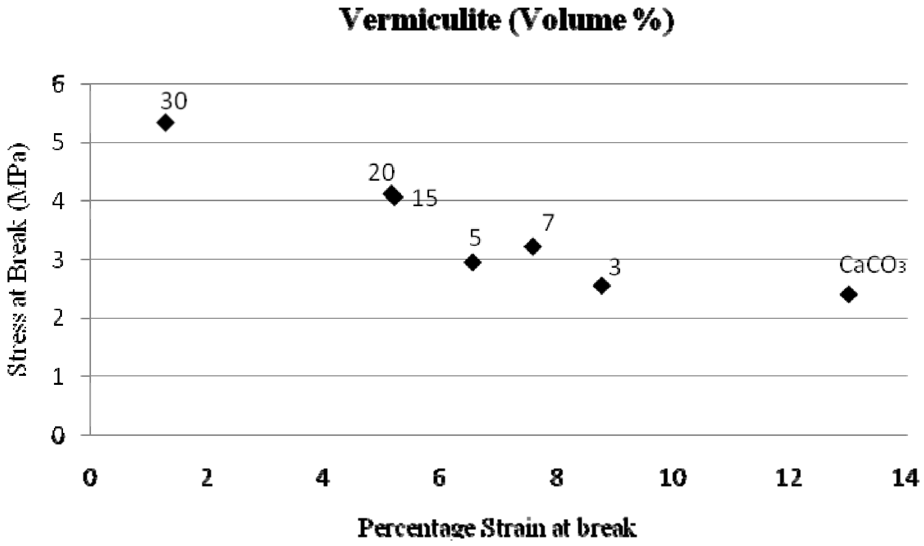

Figure 3.21 Stress- strain at break values of 3, 5, 15, 20 and 30% Vermiculite composites

Figure 3.21 above displays that when vermiculite content was increased in compositions, stress values have generally increased. 30% vermiculite content has the highest stress at break but the lowest strain. The mixing process could not be done above 30% vermiculite, since blends were crumbled into the pieces.

Figure 3.22 shows the effects of compositions on Young's modulus. Young's moduli of MnO_2 blends have almost the same values of 370 MPa. In other words, Young's modulus was not significantly affected by the addition of MnO_2 particles. Perlite content sharply increased Young's modulus. Young's moduli of baryte composites were variable. An increase in Young's modulus occurred up to 15% baryte then Young's modulus decreased. Finally, a sharp increase took place in 50% baryte composite which has Young's modulus of 543 MPa. Young's moduli of 5% - 20% vermiculite composites are close to each other at about 540 MPa, however, that of 30% vermiculite is 1062 MPa.

The comparision of the first three volume percentage of the composites (3%, 5% and 7%) indicates that perlite has the highest modulus. Increase in the tensile modulus of the material leads to increase in its brittleness. When Young's modulus of baryte and vermiculite composites are compared above 7% compositions, vermiculite compositions are less flexible. Specifically, 30% vermiculite content has the highest Young's modulus.

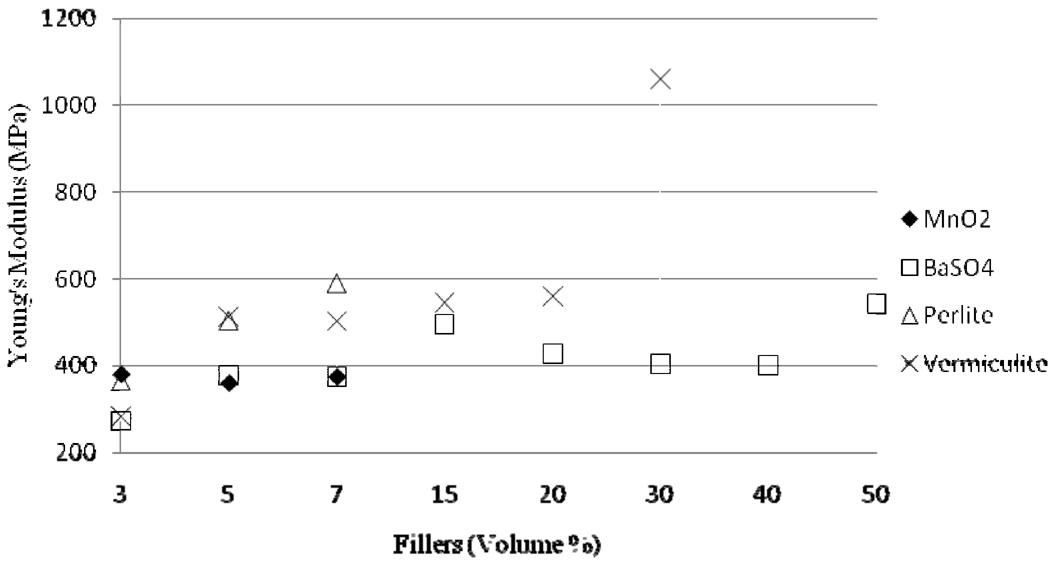

Figure 3.22 Effect of filler contents on Young's modulus

As it is shown in Figure 3.23, increase in MnO_2 and perlite contents in the bituminous composites results in a sharp increase in tensile strength. All baryte compositions are between 3 and 3.5 MPa. While the tensile strength of 3% vermiculite is the lowest which is 2.62 MPa, 30% vermiculite has the highest value at about 5.35 MPa.

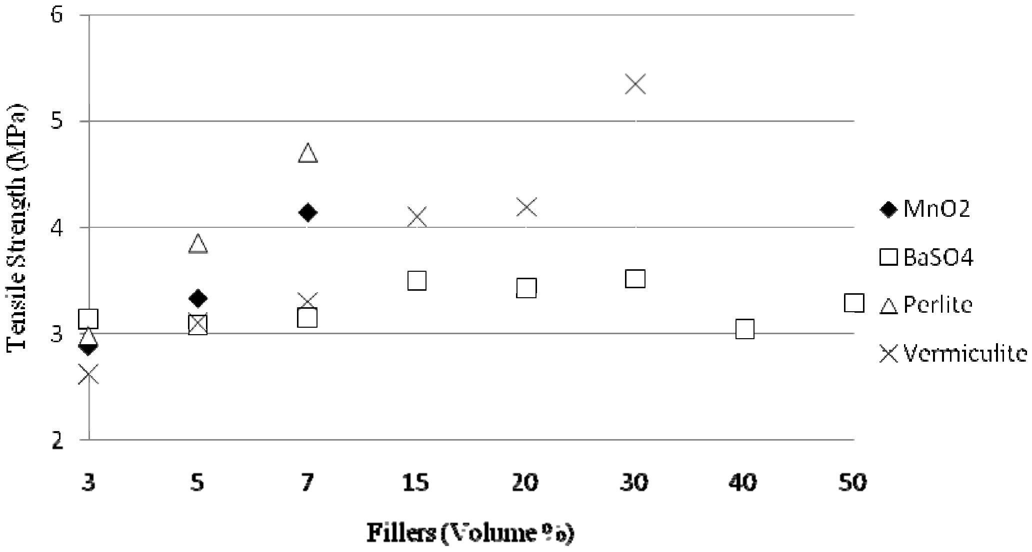

Figure 3.23 Effect of filler contents on Tensile strength

3.5 Flow Characteristics

3.5.1 Melt Flow Index (MFI)

In order to obtain information about flow characteristics of bituminous composites prepared, Melt flow index test was performed with two specified loads of 2.16 kg and 5 kg at 130°C and 2.16 kg at 150°C and 180°C. Sample containing 55% of $CaCO_3$ and no other fillers (MnO_2, $BaSO_4$, perlite and vermiculite) was taken as the reference composite. MnO_2, $BaSO_4$, perlite and vermiculite compositions were compared with $CaCO_3$ composite. For example, 3% MnO_2, $BaSO_4$, vermiculite have different MFI values at 2.16 kg and 130°C as shown in Figure 3.24. These values are compared with $CaCO_3$ which has MFI value of 1.275g/10 min.

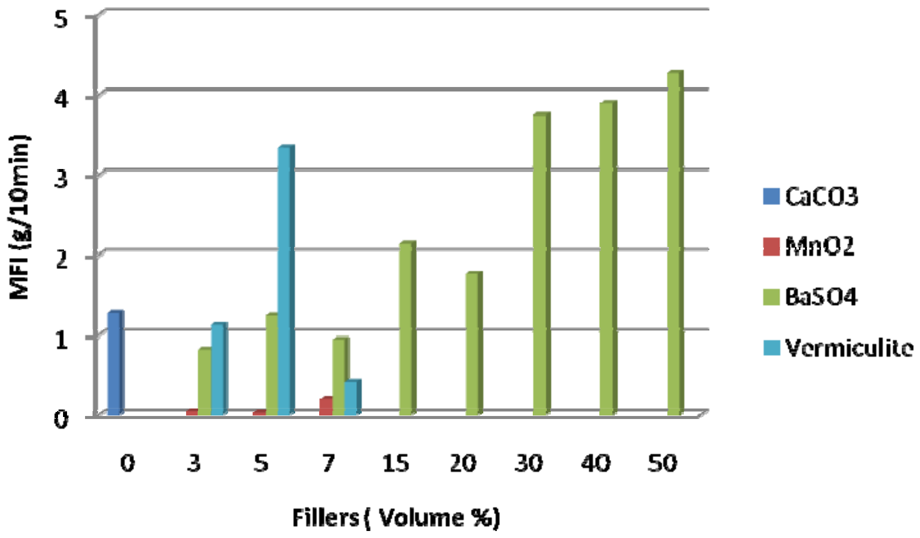

Figure 3.24 Effect of fillers and filler concentrations on melt flow index values of bituminous composites at 130°C, 2.16 kg.

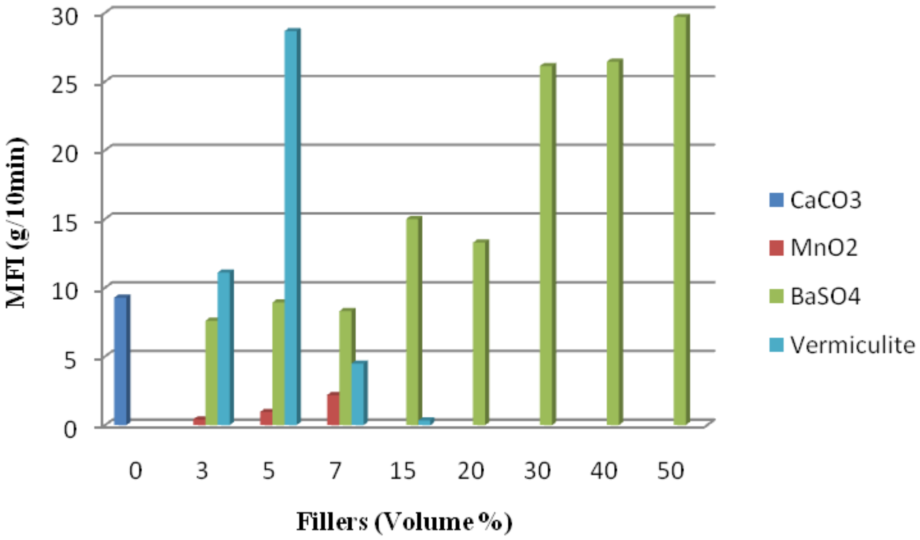

Figure 3.25 Effect of fillers and filler concentrations on melt flow index values of bituminous composites at 130°C, 5 kg.

All perlite composites did not flow at 130°C although the load was 5 kg. Therefore, perlite composites are not processible at this temperature.

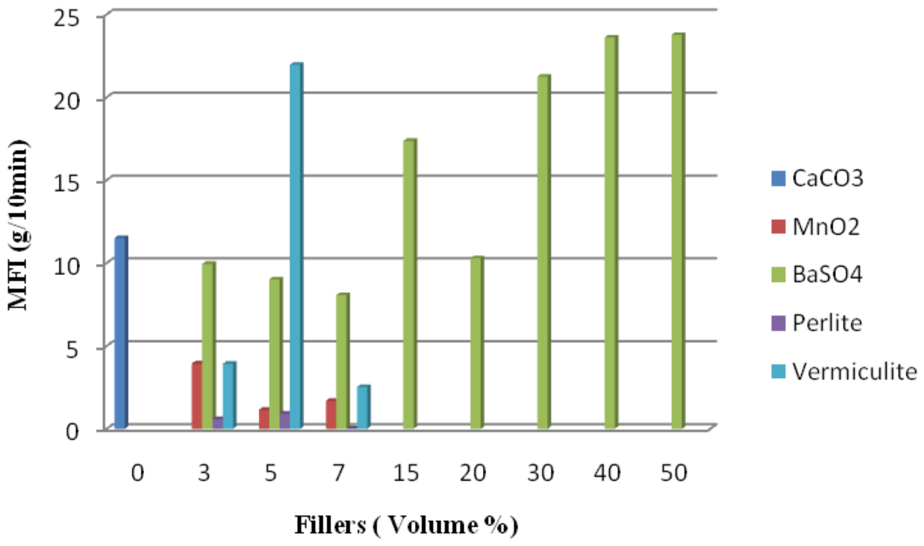

Figure 3.26 Effect of fillers and filler concentrations on melt flow index values of bituminous composites at 150°C, 2.16kg.

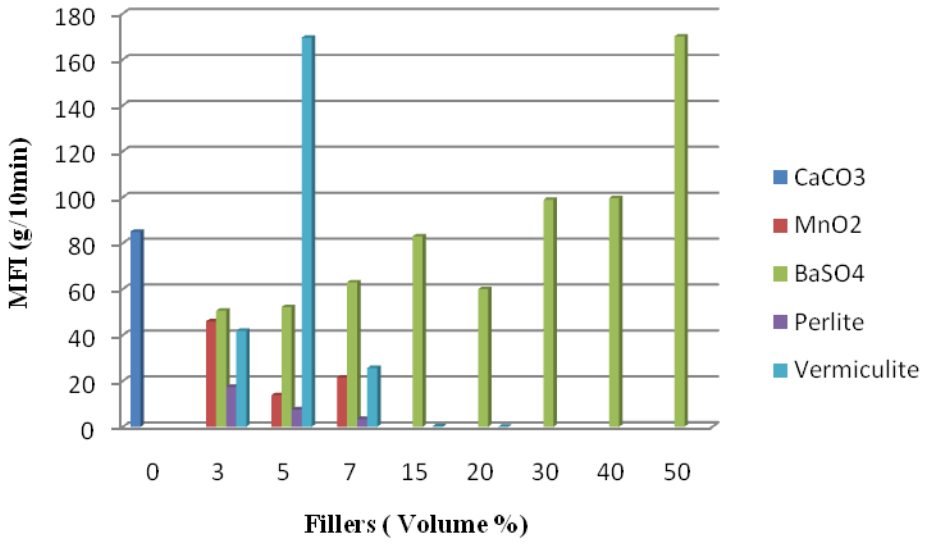

Figure 3.27 Effect of fillers and filler concentrations on melt flow index values of bituminous composites at 180°C, 2.16kg.

According to MFI results at three different temperatures, the addition of MnO_2 and perlite to the composites decreases MFI values compared to $CaCO_3$ due to their shapes and sizes. The flow may be inhibited by the agglomeration of MnO_2 particles. $BaSO_4$ has a better flowability because it is a spherical particle which flows and disperses well. In addition, $BaSO_4$ has high density and can direct the flow of composite. High baryte composites flew slowly without any load on them. The addition of $BaSO_4$ increases MFI values and 50% $BaSO_4$ composite has the highest MFI values. Although perlite did not flow at 130°C, it flew at 150°C and 180°C under 2.16 kg. However, perlite composites have the lowest MFI values, therefore using perlite in the applications can be more difficult than other fillers. 3%, 5% and 7% vermiculite composites were fluid at all temperatures. 15% vermiculite flew when the load was 5 kg at 130°C. 15% and 20% vermiculite composites flew at 180°C while 30% vermiculite was solid like at three specified temperatures. 5% vermiculite has higher MFI values than the other vermiculite composites at three temperatures since the particles can be oriented along the flow direction.

3.6 Sound Insulation Characteristics

3.6.1 Oberst Test

In order to investigate sound insulation characteristics of the bitumen based composites, Oberst test was performed at three different temperatures, 20°C, 40°C and 60°C. The test gives information about the sound damping ratio changing with frequencies. Higher damping ratio means better sound insulation. Therefore, the damping ratios of composites at all frequencies should be higher in order to get a better sound insulation material. For the dishwashers, two major noise sources were identified. While the tub lid which is excited by water jet spray during the wash and rinse portions of the cycle was the important contributor to the noise at higher frequencies from 300 Hz, pump noise emerged through the front door at lower frequencies of 200 Hz and below. The damping ratios at these frequencies should be considered while applying the composites into the diswashers. (Seperate Oberst test results for every composition were given in Appendix A).

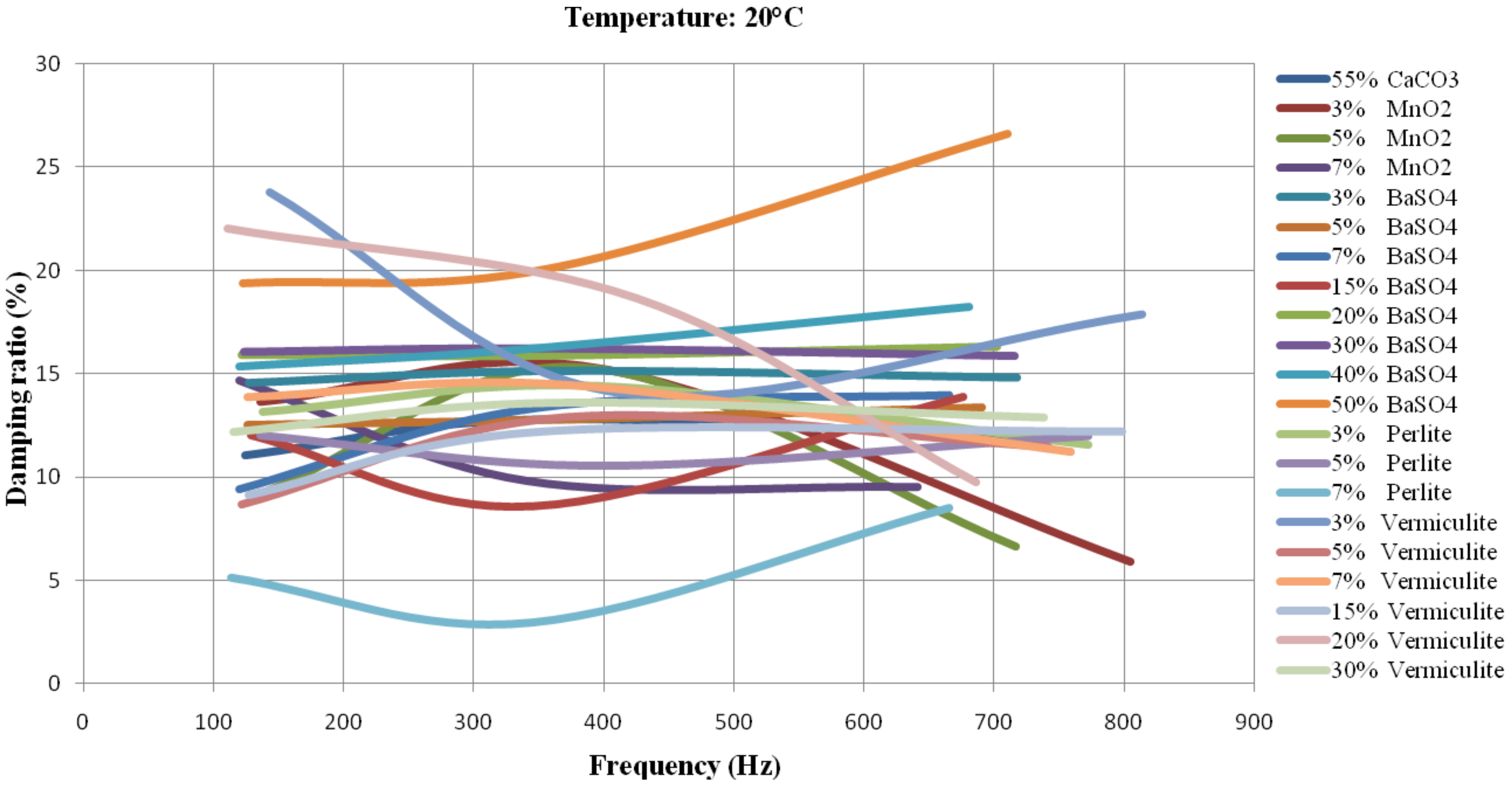

Figure 3.28 The sound damping ratio of bituminous composites changing with frequencies at 20°C.

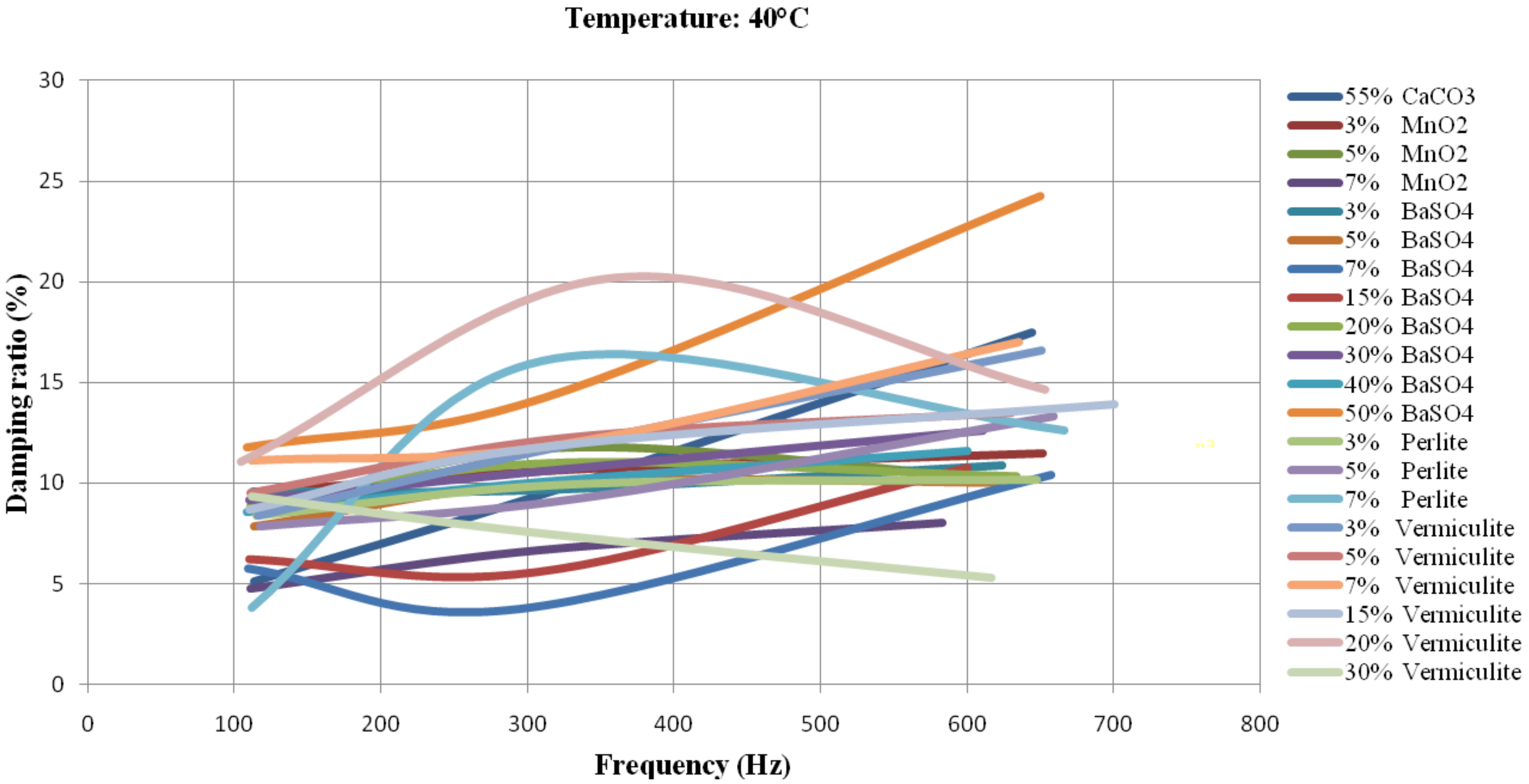

Figure 3.29 The sound damping ratio of bituminous composites changing with frequencies at 40°C.

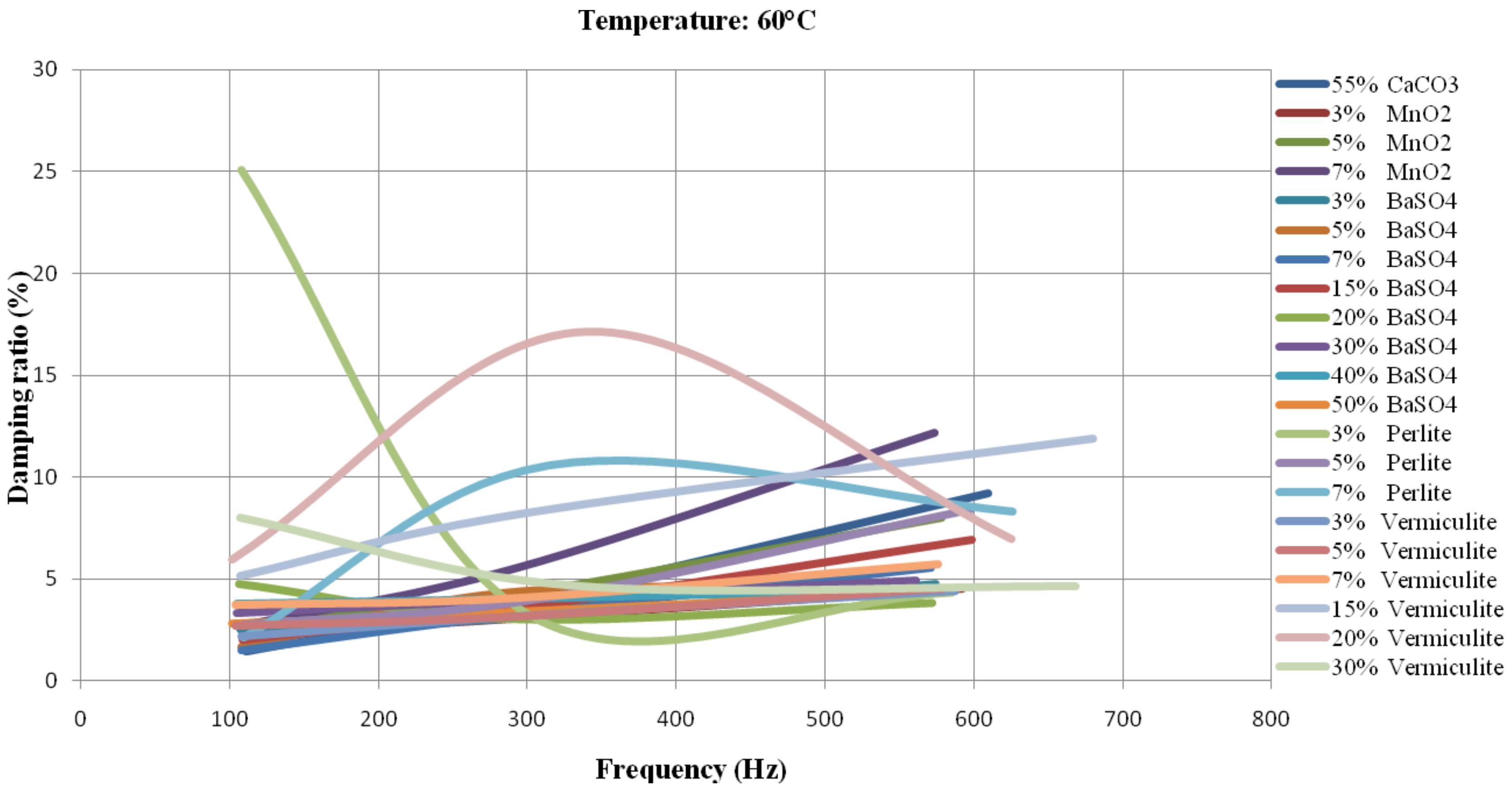

Figure 3.30 The sound damping ratio of bituminous composites changing with frequencies at 60°C.

Figure 3.28 shows the results of Oberst test at 20°C. 55% $CaCO_3$ has about 11-12 % damping ratios between 100-800 Hz. The ratios of MnO_2 composites are almost equal to that of $CaCO_3$. However, sound damping ratio of 3% MnO_2 decreases at high frequencies (about 6), though it has a better ratio at low frequencies. All baryte composites have better damping ratio than $CaCO_3$. While 3% and 5% perlite has good results in this test, 7% perlite has the lowest sound damping ratio among other composites. 3% and 20% vermiculite composites have higher results. However, the damping ratio for 20% vermiculite decreases suddenly at high frequencies. Finally, 50% baryte has the highest damping ratio which is almost twice as much as $CaCO_3$, thus, it has the highest sound insulation property.

Figure 3.29 represents the Oberst test results at 40°C. The damping ratio of 55% $CaCO_3$ is about 5.1 at lowest frequency and 17.5 at highest frequency. For $CaCO_3$ composite, damping ratio increases with an increase in frequency. 3% and 5% MnO_2 composites gave better damping ratio than $CaCO_3$ except at high frequencies, however, 7% MnO_2 composite has almost the lowest ratio. Except for 7% and 15% $BaSO_4$ composite, the damping ratios of baryte composites are higher than that of $CaCO_3$. The ratios of perlite composites are close to that of $CaCO_3$ apart from 7% perlite at high frequency. Except 30% vermiculite concentration, all vermiculite composites have good sound damping ratios which are between 10 and 15. 50% $BaSO_4$ and 20% vermiculite give the highest damping ratios at this temperature.

Figure 3.30 demonstrates the results of Oberst test at 60°C. 55% $CaCO_3$ composite has damping ratio between 1.4 at lowest frequency and 9.2 at highest frequency. MnO_2 composites give lower ratios than $CaCO_3$ composite except for 7% MnO_2 composite. The damping ratios of baryte composites are higher than that of $CaCO_3$ at low frequencies but lower at high frequencies. 3% perlite shows highest damping ratio at low frequency, however considering that such a result is so high for the perlite composite, the obtained ratio might have some deviations. The composites prepared with 15%, 20% and 30% vermiculite give better results than both $CaCO_3$ and other composites in the Oberst test, therefore, their noise insulation properties are better.

CHAPTER 4

CONCLUSIONS

The effects of four different fillers, i.e., MnO_2, $BaSO_4$, perlite and vermiculite on morphological mechanical, flowability and sound insulation characteristics of bituminous composites were studied. Adding filler to bitumen leads to reduction in the deformation produced and it results in an increase in softening point and stiffness and a decrease in penetration. The filler also increases the specific gravity of the mixture due to its high density.

All composites were prepared and presented on the basis of the volume percentage of materials. The volume percentages of bitumen, SBS and CaO were kept constant. Two different penetration grades of bitumen were used. 20/30 penetration bitumen is more viscous and harder than 50/70 penetration bitumen. In this study, while the amount of $CaCO_3$ was decreased, other fillers were added in the same proportion. The blends including MnO_2, $BaSO_4$, perlite and vermiculite were compared with 55% $CaCO_3$ composite in terms of their effectiveness and usefulness.

It is clearly observed in SEM images that all fillers were covered by bitumen. When composites including different fillers were compared with 55% $CaCO_3$ composite, stress at break values increased, however, percentage strain values decreased. MnO_2 composites had high stress but low strain at break values, thus, they were very brittle. All $BaSO_4$ specimens had close stress-strain at break values in the tensile test and all of the baryte concentrations are appropriate for the modifications of bitumen in terms of mechanical properties. Perlite composites had variability in the tensile properties. Increase in vermiculite content in the blend led to high stress but low strain at break values. According to melt flow index test, MnO_2, perlite and vermiculite composites were viscous compared to $CaCO_3$. However, 5% vermiculite composite showed a different behavior. Its high viscosity may be due to the orientation of vermiculite particles toward the flow direction. $BaSO_4$ composites were better regarding in their flow properties, hence, they may be used in the bituminous applications.

Oberst test was performed at 20°C, 40°C and 60°C to investigate the sound insulation characteristics of bituminous composites. $BaSO_4$ composites were found to have higher sound damping ratios, thus, better sound insulation characteristics at 20°C and 40°C compared to others. They still have lower damping ratios at 60°C compared to some other composites. Especially, 50% $BaSO_4$ composite has the best sound insulation property at 20°C and 40°C. Yet, sound insulation of 20% vermiculite is even better than that of $BaSO_4$ composites at 60°C.

In conclusion, MnO_2 composites seem to be worse in the measured properties. Perlite has a porous structure, but its composites did not give good results in terms of mechanical, flowability and insulation properties as we expected. 15% and 20% vermiculite composites show better insulation property but they are too viscous materials to process easily. Therefore, using vermiculite in the bituminous composite applications may not be suitable. In general, $BaSO_4$ composites have better mechanical, flow and sound insulation characteristics. 50% $BaSO_4$ composite might be used as sound insulation material because of its higher viscosity and sound damping ratio and better tensile properties.

REFERENCES

1. Parkash S., Petroleum Fuels Manufacturing Handbook, The McGraw-Hill Companies, Inc., USA, 2010.

2. Lesuer D., The Colloidal Structure of Bitumen: Consequences on the Rheology and on the Mechanisms of Bitumen Modification, *Advances in Colloid and Interface Science*, 145, 42-82, 2009.

3. Zakar P., Asphalt, Chemical Publishing Co., Newyork, 1971.

4. Abraham H., Asphalts and Allied Substances, D.Van Nostrand Company, Inc., Princeton, New Jersey, 1960.

5. Asphalt (Bitumen), International Programme on Chemical Safety, World Health Organization, Geneva, 2004.

6. Morgan P., Mulder A., The Shell Bitumen Industrial Handbook, Thomas Telford Publishing, London, 1995.

7. Robinson H.L., Polymers in Asphalt, Rapra Technology Ltd., Shawbury, Shrewsbury, Shropshire, U.K., 2004.

8. Ophart C.E., Virtual Chembook, Elmhust College, 2003.

9. Read J., Whiteoak D., The Shell Bitumen Handbook, Thomas Telford Publishing, London, 2003.

10. Amsterdam E.V., Construction Materials for Civil Engineering, Juta & Co. Ltd., Kenwyn, 2000.

11. García-Moralesa M., Partal P., Navarroa F.J., Martínez-Bozaa F., Gallegosa C., Gonzálezb N., Gonzálezb O., Muñozb M.E., Viscous Properties and Microstructure of Recycled EVA Modified Bitumen, *Fuel*, 83, 31-38, 2004.

12. Lavin P., Asphalt pavements: A practical guide to design, production and maintenance for engineers and architects, Spon Press, London, 2003.

13. Masson J.F., Polomark G.M., Bitumen microstructure by modulated differential scanning calorimetry, *Thermochimica Acta*, 374, 105-114, 2001.

14. Maquire B.W., Construction Materials, Reston Publishing Company, Inc., Reston, Va., 1981.

15. Krishnan J.M., Rajagopal K.R., Review of the uses and modeling of bitumen from ancient to modern times, *Appl. Mech. Rev.,* 56, 149-214, 2003.

16. Wauquier J.P., Petroleum Refining Volume 1: Crude Oil, Petroleum Products, Process Flowsheets, Editions Technip, Paris, 1995.

17. Gershkoff D.R., Carswell J., Nicholls J.C., Rheological Properties of Polymer-modified Binders for Use in Rolled Asphalt Wearing Course, Transport Research Laboratory Report, 1997.

18. Airey G.D., Styrene butadiene styrene polymer modification of road bitumens, *Journal of Materials Science*, 39, 951-959, 2004.

19. Ebewele R.O., Polymer Science and Technology, CRC press LLC, Florida, 2000.

20. Liu Z., Xuan M., Zhao Z., Cong Y., Liao K., A Study of the Compatibility between Asphalt and SBS, *Petroleum Science and Technology*, 21, 1317-1325, 2003.

21. Larsen D.O., Alessandrini J.L., Bosch A., Cortizo M.S., Micro-structural and rheological characteristics of SBS-asphalt blends during their manufacturing, *Construction and Building Materials*, 23, 2769-2774, 2009.

22. Sengoz B., Isikyakar G., Evaluation of the properties and microstructure of SBS and EVA polymer modified bitumen, *Construction and Building Materials*, 22, 1897-1905, 2008.

23. Shenoy A.V., Rheology of filled polymer systems, Kluwer Academic Publishers, The Neatherlands, 1999.

24. Rotron R.N., Particulate fillers for polymers, Rapra Review Reports 12, Rapra Technology Ltd., 2001.

25. DeArmitt C., Rothon R., Fillers and surface treatment, *Plastics, Additives and Compounding* , 4, 12-14, 2002.

26. Lackner R., Spiegl M., Blab R., Eberhardsteiner J., Is Low-Temperature Creep of Asphalt Mastic Independent of Filler Shape and Mineralogy?—Arguments from Multiscale Analysis, *Journal of Materials in Civil Engineering*, 17, 485-491, 2005.

27. Myers R.L., The 100 most important chemical compounds: A reference guide, Greenwood Press, Westport, 2007.

28. Edenbaum J., Plastics, Additives and Modifiers Handbook, Van Nostrand Reinhold, Newyork, 1992.

29. Wypych G., Fillers, ChemTec Publishing, Canada, 1993.

30. Pough F.H., A field guide to rocks and minerals, Peterson Field Guides, Newyork, 1995.

31. Sen D., Reference Book On Chemical Engineering, New Age International (P) Ltd., Publishers, New Delhi, 2005.

32. Seddon R., Zaworotko M., Crystal engineering: the design and application of functional solids, Kluwer Academic Publishers, The Netherlands, 1999.

33. Raghu V., Barytes : An industrially useful mineral abundantly available in India, *Resonance*, **3,** 59-61, 2008.

34. Kulshreshtha A.K., Vasile C., Handbook of polymer blends and composites, Rapra Technology Ltd., UK, 2002.

35. Gooch J.V., Encyclopedic Dictionary of Polymers, Springer, New York, 2007.

36. Somasundaran P., Encyclopedia of surface and colloid science, Second edition, Taylor and Francis Group, LLC, 2006.

37. Manukyan R.V., Davydova N.S., Perlit substrate, *Glass and Ceramics*, 54, 28-29, 1997.

38. Ciullo P.A., Industrial minerals and their uses: a handbook and formulary, Noyes Publications, USA, 1996.

39. Suvorov S.A., Skurikhin V.V., Vermiculite – A promising Material for High Temperature Heat Insulators, *Refractories and Industrial Ceramics*, 44, 44-52, 2003.

40. Mazumdar S.K., Composites Manufacturing: Materials, Product, and Process Engineering, CRC Press LLC, Florida, 2002.

41. Schärtl W., Light Scattering from Polymer Solutions and Nanoparticle Dispersions, Springer Verlag Berlin Heidelberg, Newyork, 2007.

42. Bourne G.H., Danielli J.F., International Review of Cytology Volume 30, Academic Press, Inc., London, 1971.

43. Shenoy A.V., Saini D.R., Thermoplastic melt rheology and processing, Marcel Dekker, Inc., Newyork, 1996.

44. Fasana A., Garibaldi L., Giorcelli E., Ruzzene M., Oberst beam test technique, *Proc. SPIE*, 3327**,** 451, 1998.

APPENDIX A

OBERST TEST RESULTS

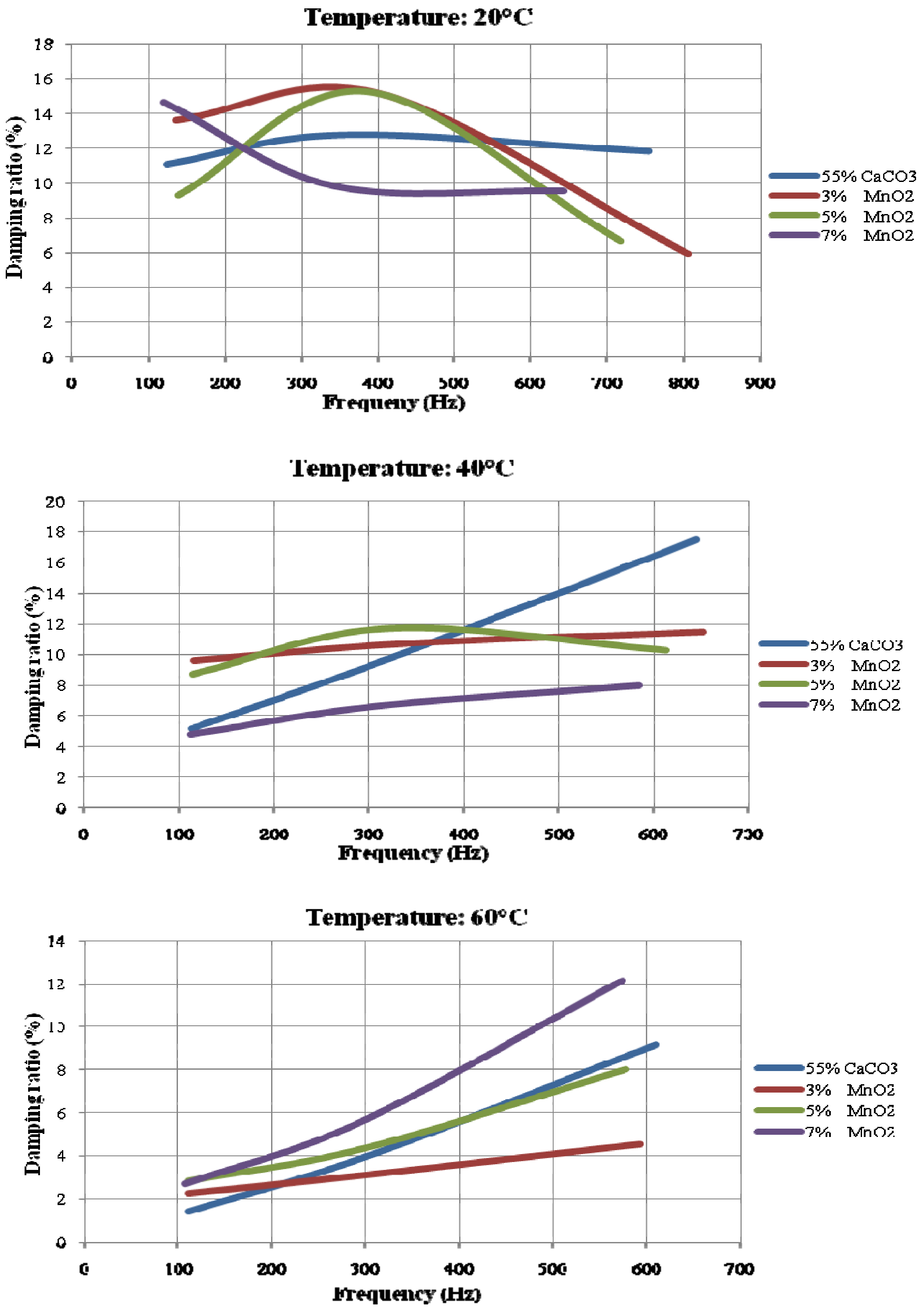

Figure A.1 Oberst test results of MnO_2 composites at 3 different temperatures

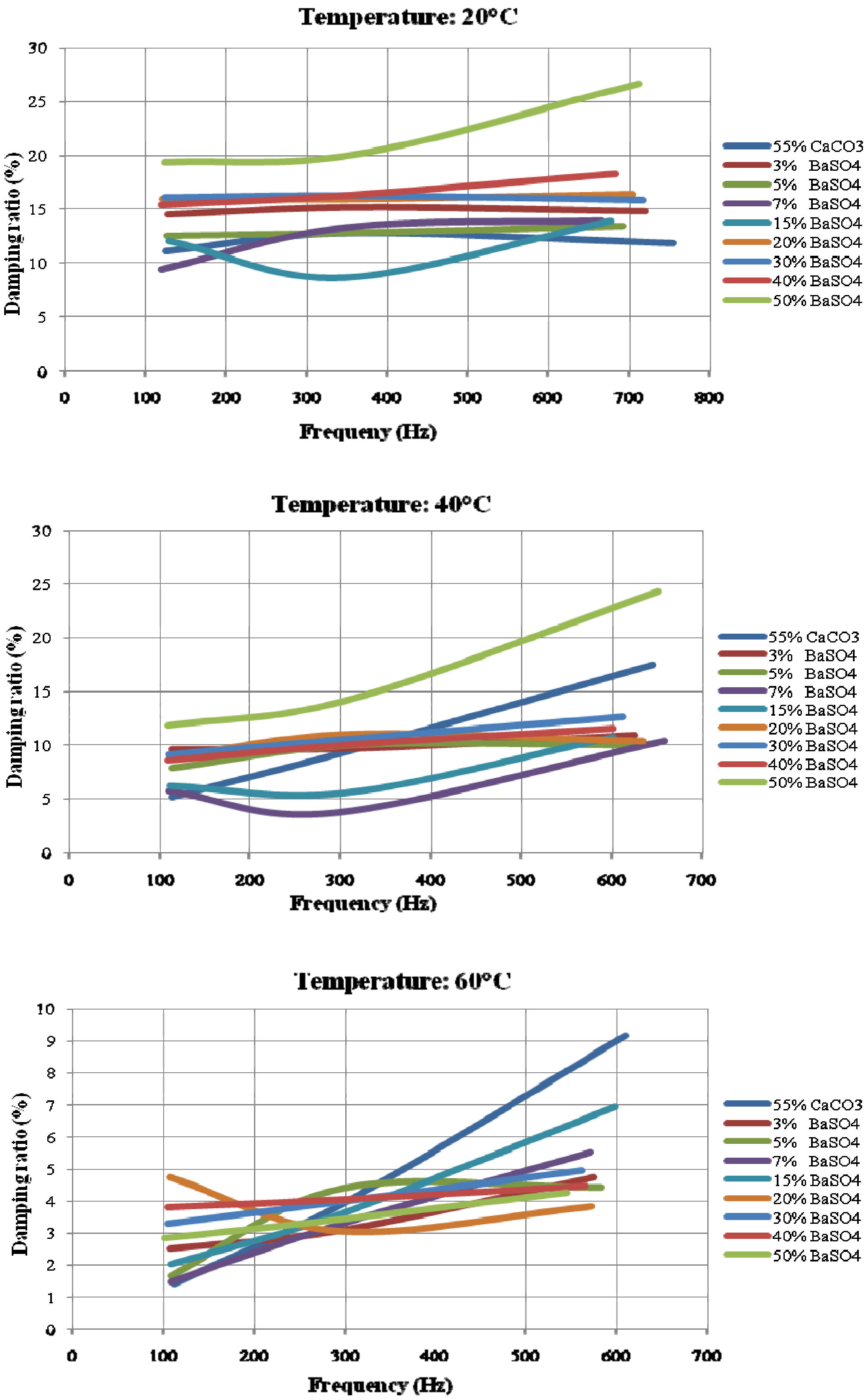

Figure A.2 Oberst test results of $BaSO_4$ composites at 3 different temperatures

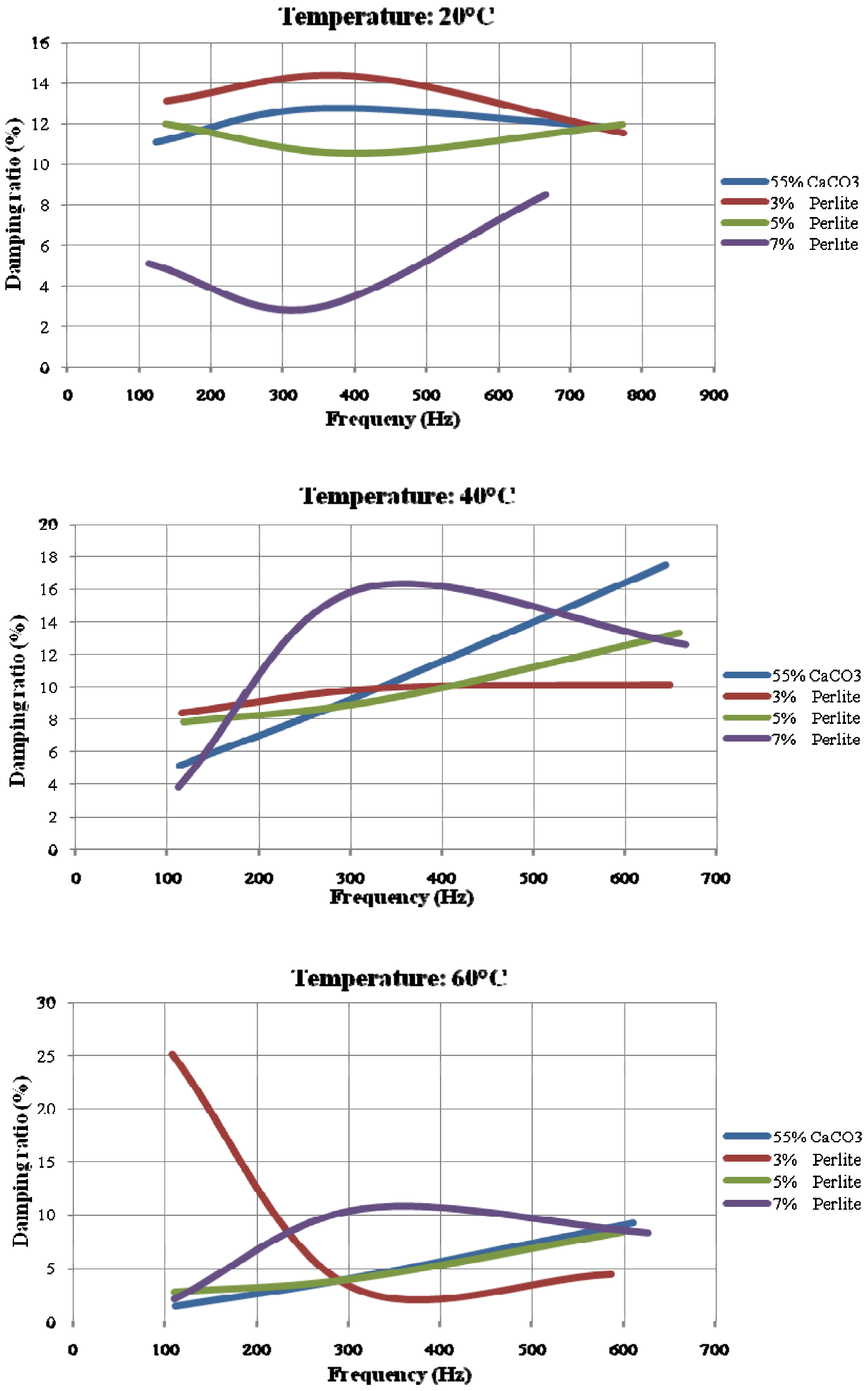

Figure A.3 Oberst test results of Perlite composites at 3 different temperatures

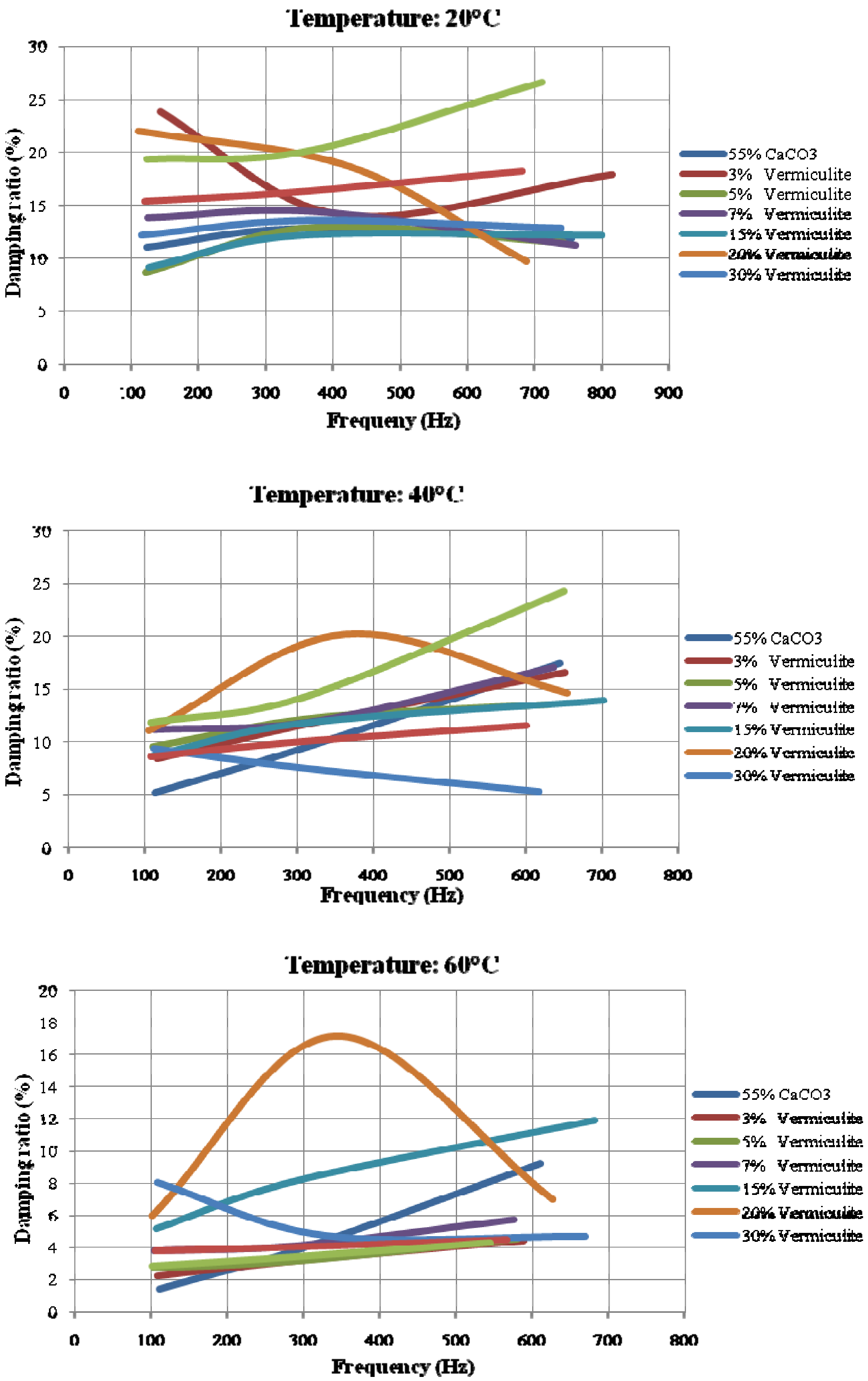

Figure A.4 Oberst test results of Vermiculite composites at 3 different temperatures

APPENDIX B

PARTICLE SIZE DISTRIBUTION HISTOGRAMS

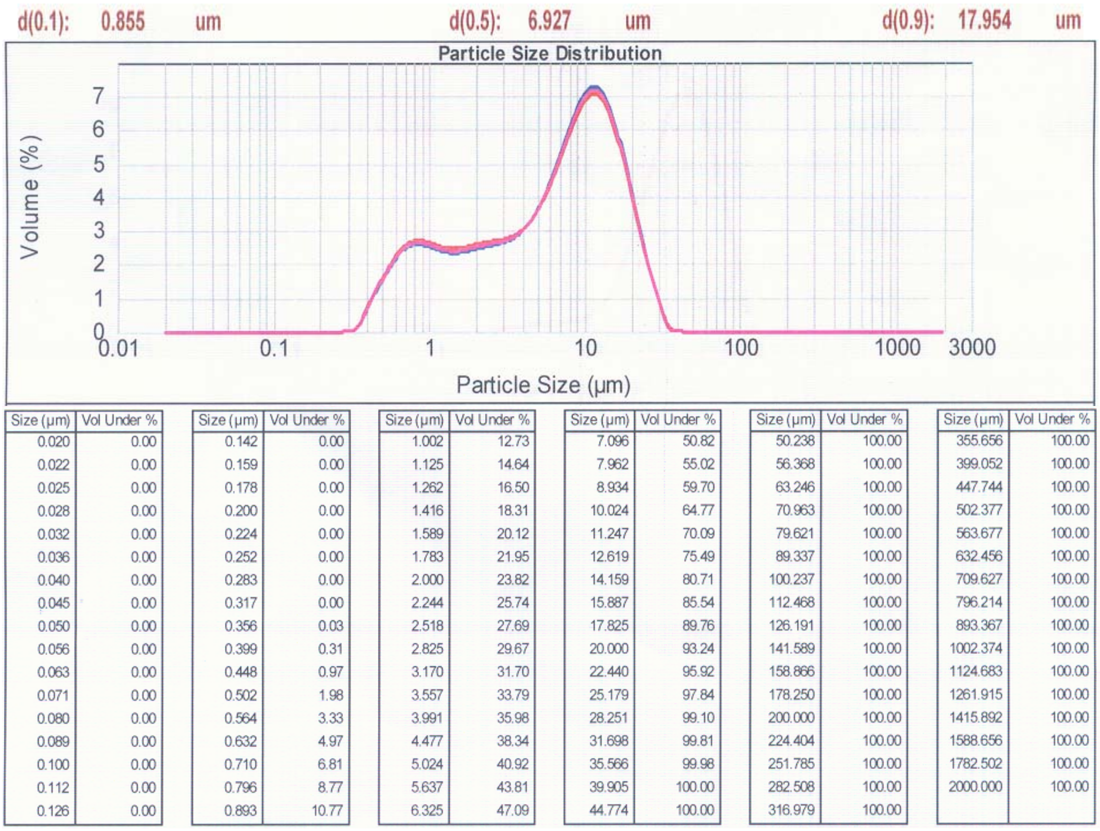

d(0.1): 0.855 um d(0.5): 6.927 um d(0.9): 17.954 um

Size (μm)	Vol Under %	Size (μm)	Vol Under %	Size (μm)	Vol Under %	Size (μm)	Vol Under %	Size (μm)	Vol Under %	Size (μm)	Vol Under %
0.020	0.00	0.142	0.00	1.002	12.73	7.096	50.82	50.238	100.00	355.656	100.00
0.022	0.00	0.159	0.00	1.125	14.64	7.962	55.02	56.368	100.00	399.052	100.00
0.025	0.00	0.178	0.00	1.262	16.50	8.934	59.70	63.246	100.00	447.744	100.00
0.028	0.00	0.200	0.00	1.416	18.31	10.024	64.77	70.963	100.00	502.377	100.00
0.032	0.00	0.224	0.00	1.589	20.12	11.247	70.09	79.621	100.00	563.677	100.00
0.036	0.00	0.252	0.00	1.783	21.95	12.619	75.49	89.337	100.00	632.456	100.00
0.040	0.00	0.283	0.00	2.000	23.82	14.159	80.71	100.237	100.00	709.627	100.00
0.045	0.00	0.317	0.00	2.244	25.74	15.887	85.54	112.468	100.00	796.214	100.00
0.050	0.00	0.356	0.03	2.518	27.69	17.825	89.76	126.191	100.00	893.367	100.00
0.056	0.00	0.399	0.31	2.825	29.67	20.000	93.24	141.589	100.00	1002.374	100.00
0.063	0.00	0.448	0.97	3.170	31.70	22.440	95.92	158.866	100.00	1124.683	100.00
0.071	0.00	0.502	1.98	3.557	33.79	25.179	97.84	178.250	100.00	1261.915	100.00
0.080	0.00	0.564	3.33	3.991	35.98	28.251	99.10	200.000	100.00	1415.892	100.00
0.089	0.00	0.632	4.97	4.477	38.34	31.698	99.81	224.404	100.00	1588.656	100.00
0.100	0.00	0.710	6.81	5.024	40.92	35.566	99.98	251.785	100.00	1782.502	100.00
0.112	0.00	0.796	8.77	5.637	43.81	39.905	100.00	282.508	100.00	2000.000	100.00
0.126	0.00	0.893	10.77	6.325	47.09	44.774	100.00	316.979	100.00		

Figure B.1 Particle size distribution histogram of $CaCO_3$

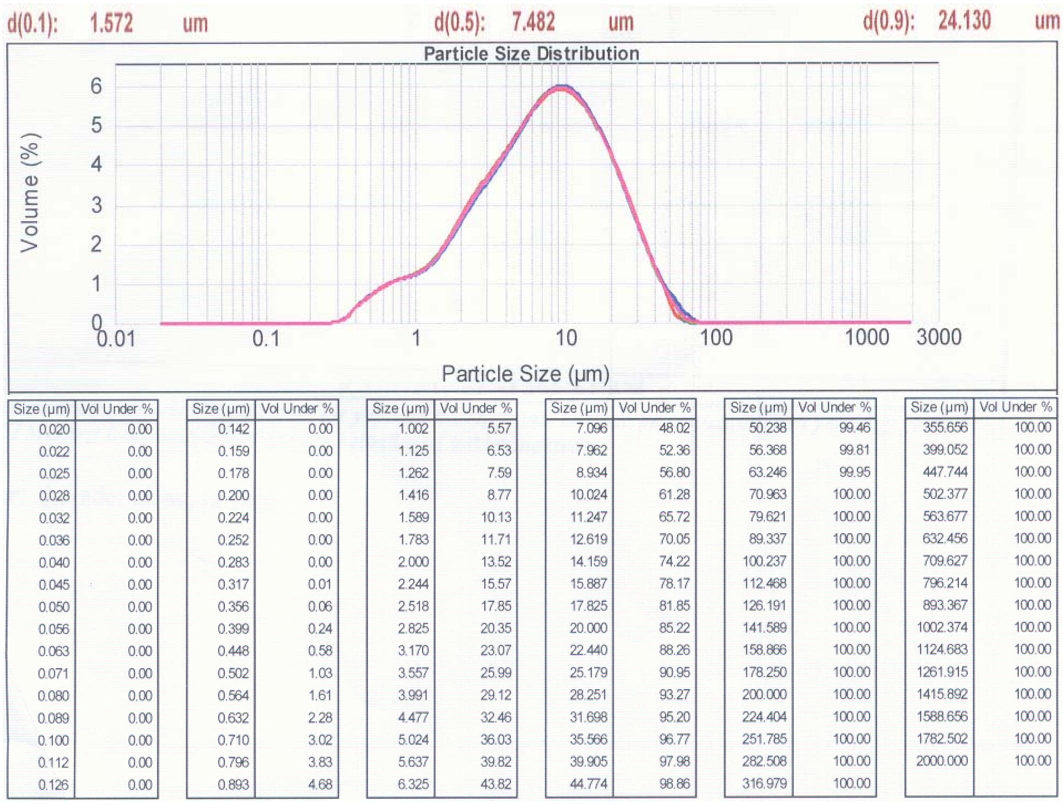

d(0.1): 1.572 um d(0.5): 7.482 um d(0.9): 24.130 um

Size (µm)	Vol Under %	Size (µm)	Vol Under %	Size (µm)	Vol Under %	Size (µm)	Vol Under %	Size (µm)	Vol Under %	Size (µm)	Vol Under %
0.020	0.00	0.142	0.00	1.002	5.57	7.096	48.02	50.238	99.46	355.656	100.00
0.022	0.00	0.159	0.00	1.125	6.53	7.962	52.36	56.368	99.81	399.052	100.00
0.025	0.00	0.178	0.00	1.262	7.59	8.934	56.80	63.246	99.95	447.744	100.00
0.028	0.00	0.200	0.00	1.416	8.77	10.024	61.28	70.963	100.00	502.377	100.00
0.032	0.00	0.224	0.00	1.589	10.13	11.247	65.72	79.621	100.00	563.677	100.00
0.036	0.00	0.252	0.00	1.783	11.71	12.619	70.05	89.337	100.00	632.456	100.00
0.040	0.00	0.283	0.00	2.000	13.52	14.159	74.22	100.237	100.00	709.627	100.00
0.045	0.00	0.317	0.01	2.244	15.57	15.887	78.17	112.468	100.00	796.214	100.00
0.050	0.00	0.356	0.06	2.518	17.85	17.825	81.85	126.191	100.00	893.367	100.00
0.056	0.00	0.399	0.24	2.825	20.35	20.000	85.22	141.589	100.00	1002.374	100.00
0.063	0.00	0.448	0.58	3.170	23.07	22.440	88.26	158.866	100.00	1124.683	100.00
0.071	0.00	0.502	1.03	3.557	25.99	25.179	90.95	178.250	100.00	1261.915	100.00
0.080	0.00	0.564	1.61	3.991	29.12	28.251	93.27	200.000	100.00	1415.892	100.00
0.089	0.00	0.632	2.28	4.477	32.46	31.698	95.20	224.404	100.00	1588.656	100.00
0.100	0.00	0.710	3.02	5.024	36.03	35.566	96.77	251.785	100.00	1782.502	100.00
0.112	0.00	0.796	3.83	5.637	39.82	39.905	97.98	282.508	100.00	2000.000	100.00
0.126	0.00	0.893	4.68	6.325	43.82	44.774	98.86	316.979	100.00		

Figure B.2 Particle size distribution histogram of MnO_2

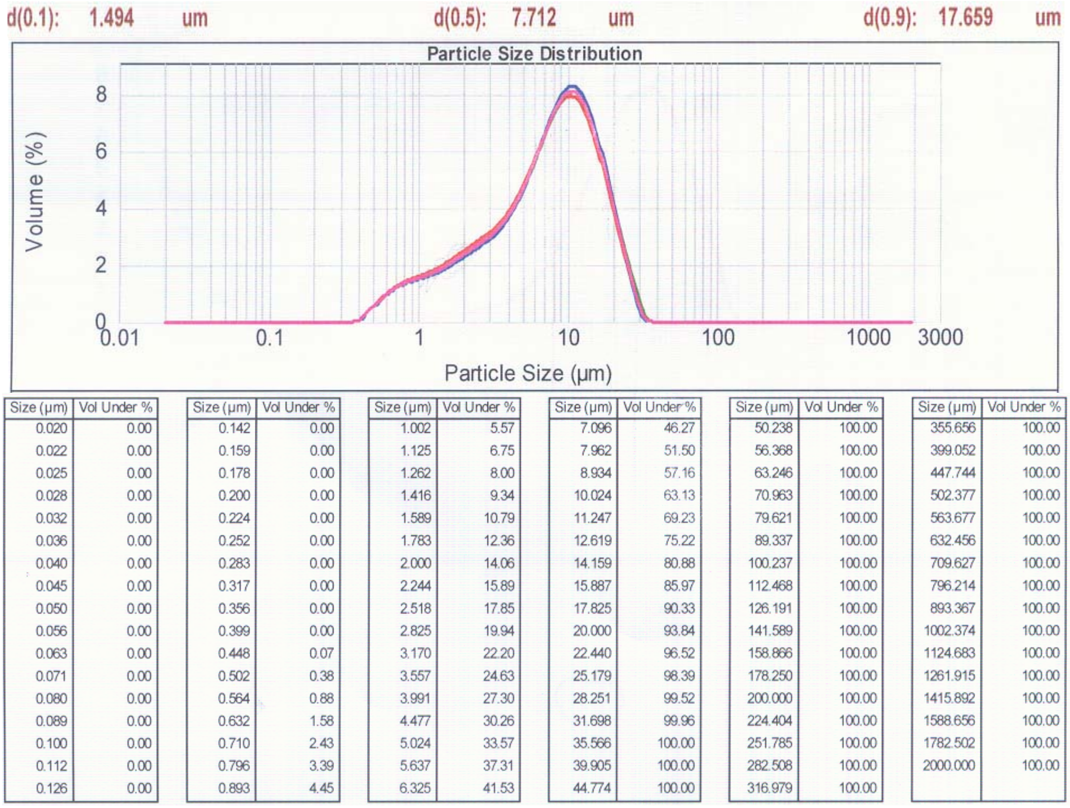

d(0.1): 1.494 um d(0.5): 7.712 um d(0.9): 17.659 um

Size (µm)	Vol Under %	Size (µm)	Vol Under %	Size (µm)	Vol Under %	Size (µm)	Vol Under %	Size (µm)	Vol Under %	Size (µm)	Vol Under %
0.020	0.00	0.142	0.00	1.002	5.57	7.096	46.27	50.238	100.00	355.656	100.00
0.022	0.00	0.159	0.00	1.125	6.75	7.962	51.50	56.368	100.00	399.052	100.00
0.025	0.00	0.178	0.00	1.262	8.00	8.934	57.16	63.246	100.00	447.744	100.00
0.028	0.00	0.200	0.00	1.416	9.34	10.024	63.13	70.963	100.00	502.377	100.00
0.032	0.00	0.224	0.00	1.589	10.79	11.247	69.23	79.621	100.00	563.677	100.00
0.036	0.00	0.252	0.00	1.783	12.36	12.619	75.22	89.337	100.00	632.456	100.00
0.040	0.00	0.283	0.00	2.000	14.06	14.159	80.88	100.237	100.00	709.627	100.00
0.045	0.00	0.317	0.00	2.244	15.89	15.887	85.97	112.468	100.00	796.214	100.00
0.050	0.00	0.356	0.00	2.518	17.85	17.825	90.33	126.191	100.00	893.367	100.00
0.056	0.00	0.399	0.00	2.825	19.94	20.000	93.84	141.589	100.00	1002.374	100.00
0.063	0.00	0.448	0.07	3.170	22.20	22.440	96.52	158.866	100.00	1124.683	100.00
0.071	0.00	0.502	0.38	3.557	24.63	25.179	98.39	178.250	100.00	1261.915	100.00
0.080	0.00	0.564	0.88	3.991	27.30	28.251	99.52	200.000	100.00	1415.892	100.00
0.089	0.00	0.632	1.58	4.477	30.26	31.698	99.96	224.404	100.00	1588.656	100.00
0.100	0.00	0.710	2.43	5.024	33.57	35.566	100.00	251.785	100.00	1782.502	100.00
0.112	0.00	0.796	3.39	5.637	37.31	39.905	100.00	282.508	100.00	2000.000	100.00
0.126	0.00	0.893	4.45	6.325	41.53	44.774	100.00	316.979	100.00		

Figure B.3 Particle size distribution histogram of $BaSO_4$

d(0.1): 8.340 um d(0.5): 28.133 um d(0.9): 68.642 um

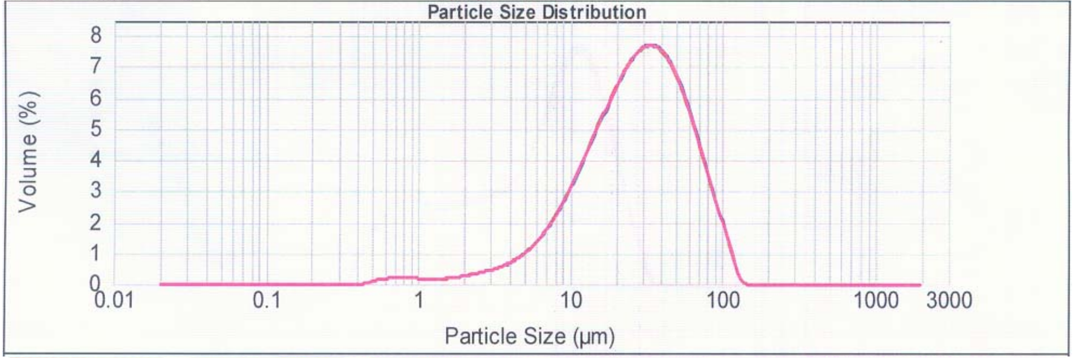

Size (μm)	Vol Under %	Size (μm)	Vol Under %	Size (μm)	Vol Under %	Size (μm)	Vol Under %	Size (μm)	Vol Under %	Size (μm)	Vol Under %
0.020	0.00	0.142	0.00	1.002	0.80	7.096	7.84	50.238	78.21	355.656	100.00
0.022	0.00	0.159	0.00	1.125	0.92	7.962	9.32	56.368	83.01	399.052	100.00
0.025	0.00	0.178	0.00	1.262	1.04	8.934	11.10	63.246	87.31	447.744	100.00
0.028	0.00	0.200	0.00	1.416	1.16	10.024	13.22	70.963	91.00	502.377	100.00
0.032	0.00	0.224	0.00	1.589	1.28	11.247	15.71	79.621	94.07	563.677	100.00
0.036	0.00	0.252	0.00	1.783	1.43	12.619	18.59	89.337	96.49	632.456	100.00
0.040	0.00	0.283	0.00	2.000	1.60	14.159	21.90	100.237	98.28	709.627	100.00
0.045	0.00	0.317	0.00	2.244	1.81	15.887	25.64	112.468	99.44	796.214	100.00
0.050	0.00	0.356	0.00	2.518	2.05	17.825	29.80	126.191	99.96	893.367	100.00
0.056	0.00	0.399	0.00	2.825	2.33	20.000	34.39	141.589	100.00	1002.374	100.00
0.063	0.00	0.448	0.00	3.170	2.67	22.440	39.35	158.866	100.00	1124.683	100.00
0.071	0.00	0.502	0.02	3.557	3.06	25.179	44.65	178.250	100.00	1261.915	100.00
0.080	0.00	0.564	0.11	3.991	3.53	28.251	50.21	200.000	100.00	1415.892	100.00
0.089	0.00	0.632	0.23	4.477	4.09	31.698	55.93	224.404	100.00	1588.656	100.00
0.100	0.00	0.710	0.37	5.024	4.77	35.566	61.71	251.785	100.00	1782.502	100.00
0.112	0.00	0.796	0.51	5.637	5.60	39.905	67.44	282.508	100.00	2000.000	100.00
0.126	0.00	0.893	0.66	6.325	6.61	44.774	72.97	316.979	100.00		

Figure B.4 Particle size distribution histogram of Perlite

d(0.1): 12.662 um d(0.5): 48.304 um d(0.9): 116.111 um

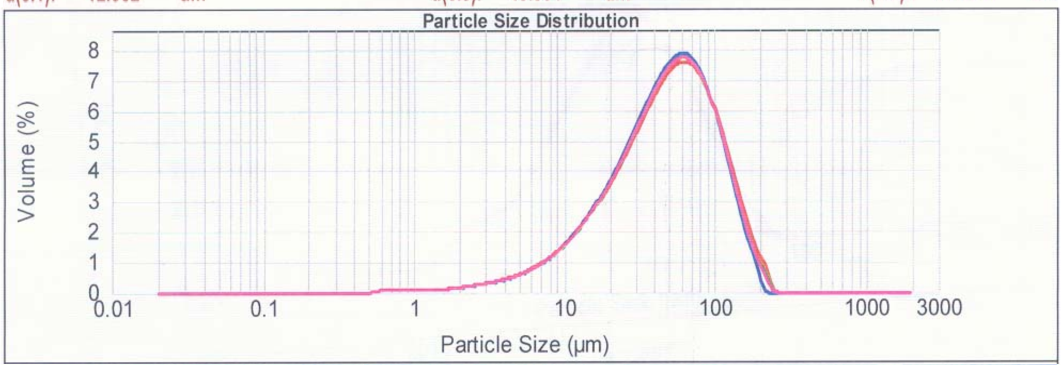

Size (μm)	Vol Under %	Size (μm)	Vol Under %	Size (μm)	Vol Under %	Size (μm)	Vol Under %	Size (μm)	Vol Under %	Size (μm)	Vol Under %
0.020	0.00	0.142	0.00	1.002	0.32	7.096	4.46	50.238	51.89	355.656	100.00
0.022	0.00	0.159	0.00	1.125	0.38	7.962	5.24	56.368	57.57	399.052	100.00
0.025	0.00	0.178	0.00	1.262	0.44	8.934	6.16	63.246	63.38	447.744	100.00
0.028	0.00	0.200	0.00	1.416	0.50	10.024	7.23	70.963	69.16	502.377	100.00
0.032	0.00	0.224	0.00	1.589	0.56	11.247	8.49	79.621	74.76	563.677	100.00
0.036	0.00	0.252	0.00	1.783	0.65	12.619	9.95	89.337	80.03	632.456	100.00
0.040	0.00	0.283	0.00	2.000	0.76	14.159	11.64	100.237	84.81	709.627	100.00
0.045	0.00	0.317	0.00	2.244	0.89	15.887	13.59	112.468	88.97	796.214	100.00
0.050	0.00	0.356	0.00	2.518	1.05	17.825	15.82	126.191	92.43	893.367	100.00
0.056	0.00	0.399	0.00	2.825	1.24	20.000	18.36	141.589	95.16	1002.374	100.00
0.063	0.00	0.448	0.00	3.170	1.46	22.440	21.23	158.866	97.18	1124.683	100.00
0.071	0.00	0.502	0.00	3.557	1.72	25.179	24.46	178.250	98.57	1261.915	100.00
0.080	0.00	0.564	0.00	3.991	2.01	28.251	28.08	200.000	99.44	1415.892	100.00
0.089	0.00	0.632	0.06	4.477	2.36	31.698	32.08	224.404	99.91	1588.656	100.00
0.100	0.00	0.710	0.12	5.024	2.77	35.566	36.49	251.785	100.00	1782.502	100.00
0.112	0.00	0.796	0.20	5.637	3.24	39.905	41.28	282.508	100.00	2000.000	100.00
0.126	0.00	0.893	0.26	6.325	3.80	44.774	46.43	316.979	100.00		

Figure B.5 Particle size distribution histogram of Vermiculite